



HUMAN HEALTH

ENVIRONMENTAL HEALTH

FOOD ADDITIVES AND INGREDIENTS

Food Additives and Ingredients Compendium


PerkinElmer[®]
For the Better



FOOD ADDITIVES AND INGREDIENTS

Table of Contents

Food Additives and Ingredients

Simultaneous Analysis of Nine Food Additives with the PerkinElmer Flexar FX-15 System Equipped with a PDA Detector	3
Analysis of Color Additives in Beverages with the PerkinElmer Flexar FX-15 System Equipped with a PDA Detector	7
Analysis of Common Sweeteners and Additives in Beverages with the PerkinElmer Flexar FX-15 System Equipped with a PDA Detector	11
Dissolution of Gelatin Monitored by DMA	16
Increased Throughput and Reduced Solvent Consumption for the Determination of Isoflavones by UHPLC	18
Using the D-Swafer to Investigate Solvent Impurities by Heartcutting GC/MS	22
Investigation of Amorphous Sucrose Using Material Pockets and Humidity Generator	29
Detection of Honey Adulteration Using FT-NIR Spectroscopy	31
Analysis of Sugars in Honey Using the PerkinElmer Altus HPLC System with RI Detection	35
Characterizing the Hydrothermal Behavior of Starch with Dynamic Mechanical Analysis	40
Qualifying Mustard Flavor by Headspace Trap GC/MS using the Clarus SQ 8	45
The Use of FT-IR Spectroscopy as a Technique for Verifying Maple Syrup Authenticity	48
The Qualitative and Quantitative Analysis of Steviol Glycosides by HPLC- PDA in Energy/Vitamin Drinks	51

UHPLC

Author**Njies Pedjie****PerkinElmer, Inc.
Shelton, CT 06484 USA**

Simultaneous Analysis of Nine Food Additives with the PerkinElmer Flexar FX-15 System Equipped with a PDA Detector

Introduction

Food additives are natural or synthetic substances that are added in food, beverage and pharmaceutical products for their microbicidal, preservative and flavoring properties. Among the commonly used additives, benzoic acid and its salts are widely used in beverage and food for preservation. Artificial sweeteners are widely used as sugar substitute in calorie-conscious societies, where their intake provides practically no calories and also helps fight obesity and its related ailments.

In most countries, the use of additives is regulated. In the U.S., most additives are part of the Generally Recognized As Safe (GRAS) ingredients although the FDA has established Acceptable Daily Intake (ADI) for each of them. There is a need for analytical techniques to identify and quantify additives because the food industry is required to list the type and amount of each ingredient on product labels to help consumers make dietary choices and manage food allergies.

This application note presents a fast and robust liquid chromatography method to simultaneously test nine widely used additives. Among the additives tested are: preservatives (benzoic acid, sorbic acid, dehydroacetic acid and methylparaben); artificial sweeteners (acesulfame potassium, saccharin and aspartame); flavoring agent (quinine); and a stimulant (caffeine). Method conditions and performance data including precision, accuracy and linearity are presented. The method is applied to a mouthwash and a tonic soda and the type and amount of additives are confirmed.

Experimental

Nine stock standard solutions of each additive at 1 mg/mL concentration were prepared by dilution with water, followed by one minute vortex and five minutes sonication. A working standard of 0.1 mg/mL was prepared by transferring one mL of each of the stock solution into 10 mL volumetric flask. The solution was brought to volume with water and mixed well.

Precision was evaluated with five injections of the working standard. Linearity was determined across a range of 2.5 – 100 µg/mL. To assess accuracy, purified water was spiked with the working standard to obtain a 0.005 mg/mL solution. About 0.25 g/mL of a popular mouthwash and 0.5 g/mL of a tonic soda was prepared by dilution with water. The solutions were thoroughly mixed and filtered with a 0.2 µm nylon membrane prior to testing.

A PerkinElmer® Flexar™ FX-15 UHPLC system fitted with a Flexar FX PDA (photodiode array detector) served as a platform for this experiment. The separation was achieved using a PerkinElmer Brownlee SPP C-18, 50 x 2.1 mm, 2.7 µm (superficially porous particle) column.

Table 1. Detailed UHPLC system and chromatographic conditions.

Autosampler:	Flexar FX UHPLC												
	Setting: 50 µL loop and 15 µL needle volume, partial loop mode, 350 µL mixer												
	Injection: 2 µL; injector wash and carrier: water												
PDA Detector:	Scanned from 190 – 400 nm, recording setting 214 nm												
UHPLC Column:	PerkinElmer Brownlee SPP C-18, 50 x 2.1 mm 2.7 µm (superficially porous particles) at 45 °C, Part No. N9308402												
Mobile Phase:	A: 20 mM sodium acetate in water adjusted to pH 4.57 with acetic acid												
	B: acetonitrile												
	<table><tr><th>Time (min)</th><th>Flow rate (mL/min)</th><th>B %</th><th>Curve</th></tr><tr><td>6</td><td>0.4</td><td>5-30</td><td>1</td></tr><tr><td>1</td><td>0.4</td><td>40</td><td>1</td></tr></table>	Time (min)	Flow rate (mL/min)	B %	Curve	6	0.4	5-30	1	1	0.4	40	1
Time (min)	Flow rate (mL/min)	B %	Curve										
6	0.4	5-30	1										
1	0.4	40	1										
	3 minutes equilibration after each run (HPLC grade solvent and ACS grade reagent)												
Sampling Rate:	5 pts/s												
Software:	Chromera® Version 3.0												

Results And Discussion

The optimal flow rate of this method was determined to be 0.4 mL/min. at 45 °C and the pressure stabilized around 5500 PSI. All the peaks eluted within seven minutes. Prior to running the samples, from one injection of the working standard solution, the maximum wavelength of each peak was determined and the wavelength setting was optimized (see Figure 1, 2). The chromatogram of a popular mouthwash tested is presented in Figure 3. Excellent method performance was achieved: the linearity of the analysis shows a R-squared of not less than 0.997 for each additive, and a precision relative standard deviation (%RSD) average of 0.84% with values ranging from 0.47% to 1.37%. The spiked purified water tested has an average recovery of 97.1% with value ranging from 91.3% to 108.7%. Details of the method performance and results of the samples tested are presented in Table 2.

Although in liquid chromatography peak identification is usually based on the retention time, Chromera's ability to collect and store spectra (Figure 4) offers another way of identification by matching any peak spectrum to spectra stored in its library. This feature of Chromera adds another level of confidence in the analysis as the same relative retention time does not necessarily mean the components are the same. Confirmation of the presence of aspartame and quinine in the tonic soda sample is shown in Figure 5. In that figure, spectra at the peak apexes are compared to the spectra stored in the library. When a match is made, the name of the matching spectrum appears on each peak in question, confirming its identity.

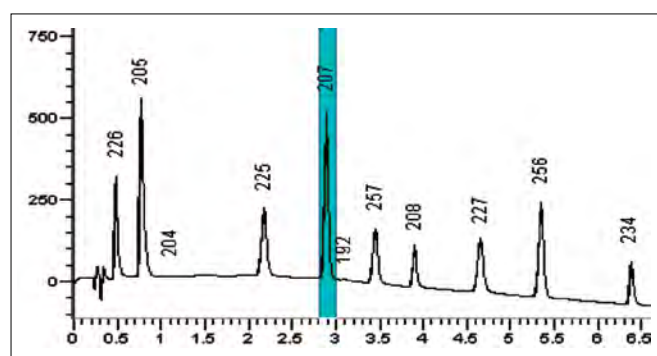


Figure 1. Chromatogram from the analyses of the standard solution with the maximum absorbance for each peak.

Table 1. Precision, linearity, accuracy and samples.

Compound	%RSD	r ²	Range (µg/mL)	Mouthwash (mg/12 oz)	Tonic Soda (mg/12 oz)	Spiked Recovery %
Acesulfame K	1.33	0.9997	2.5 – 100	ND	ND	108.7
Saccharine	0.88	0.9999	2.5 – 100	151	ND	94.1
Benzoic Acid	1.12	1	5.0 – 100	177	ND	93.1
Caffeine	0.57	0.9994	2.5 – 100	ND	ND	97.0
Sorbic Acid	0.80	0.9991	2.5 – 100	ND	ND	94.6
Aspartame	1.14	0.9965	5.0 – 100	ND	117	94.9
Dehydroacetic Acid	0.76	0.9994	5.0 – 100	ND	ND	99.5
Methylparaben	0.54	0.9999	2.5 – 100	ND	ND	100.3
Quinine	0.47	0.9967	5.0 – 100	ND	69	91.3
Average	0.85	0.9990	NA	NA	NA	97.1

ND = None detected NA = Not applicable

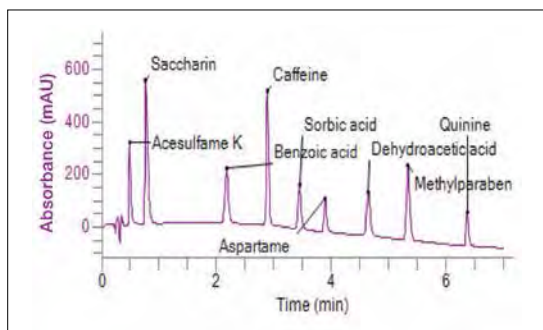


Figure 2. Chromatogram from the analysis of the standard solution.

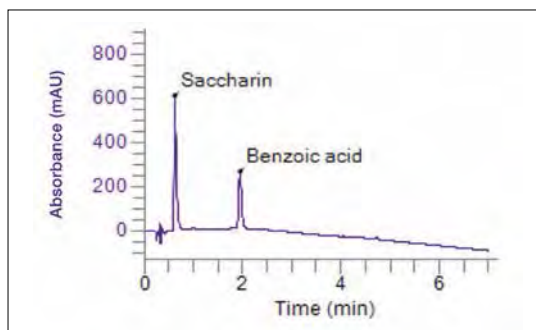


Figure 3. Chromatogram from the analyses of a popular mouthwash.

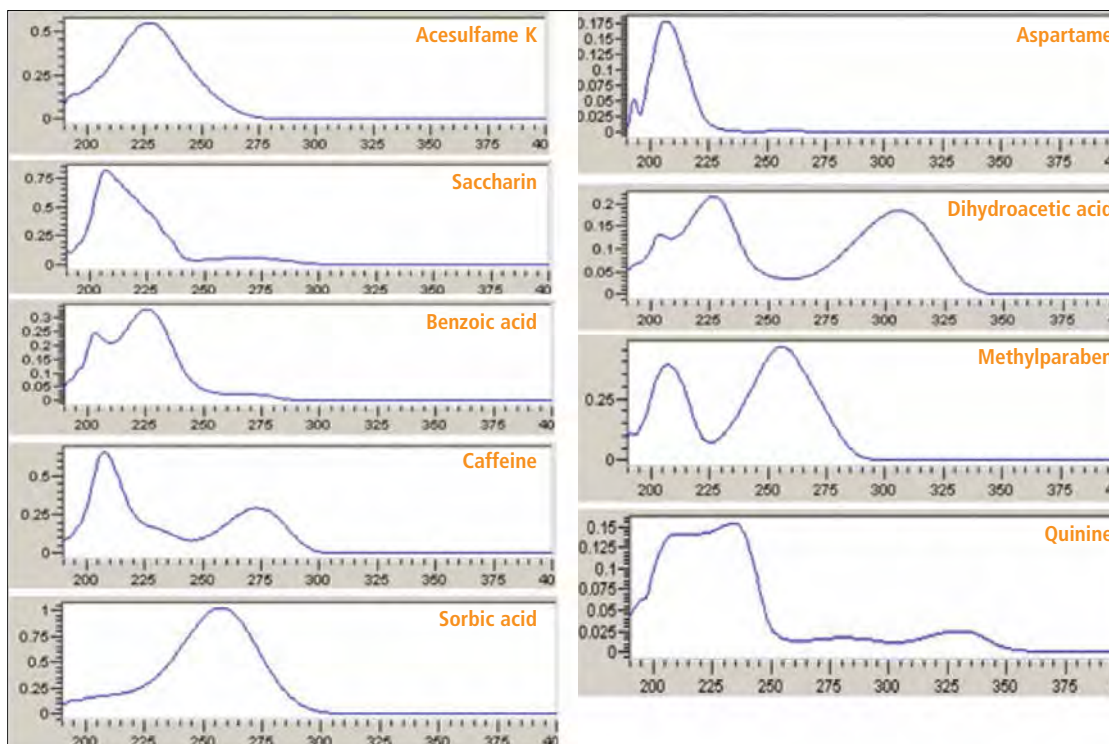


Figure 4. Spectra of the additives from the standard solution analysis.

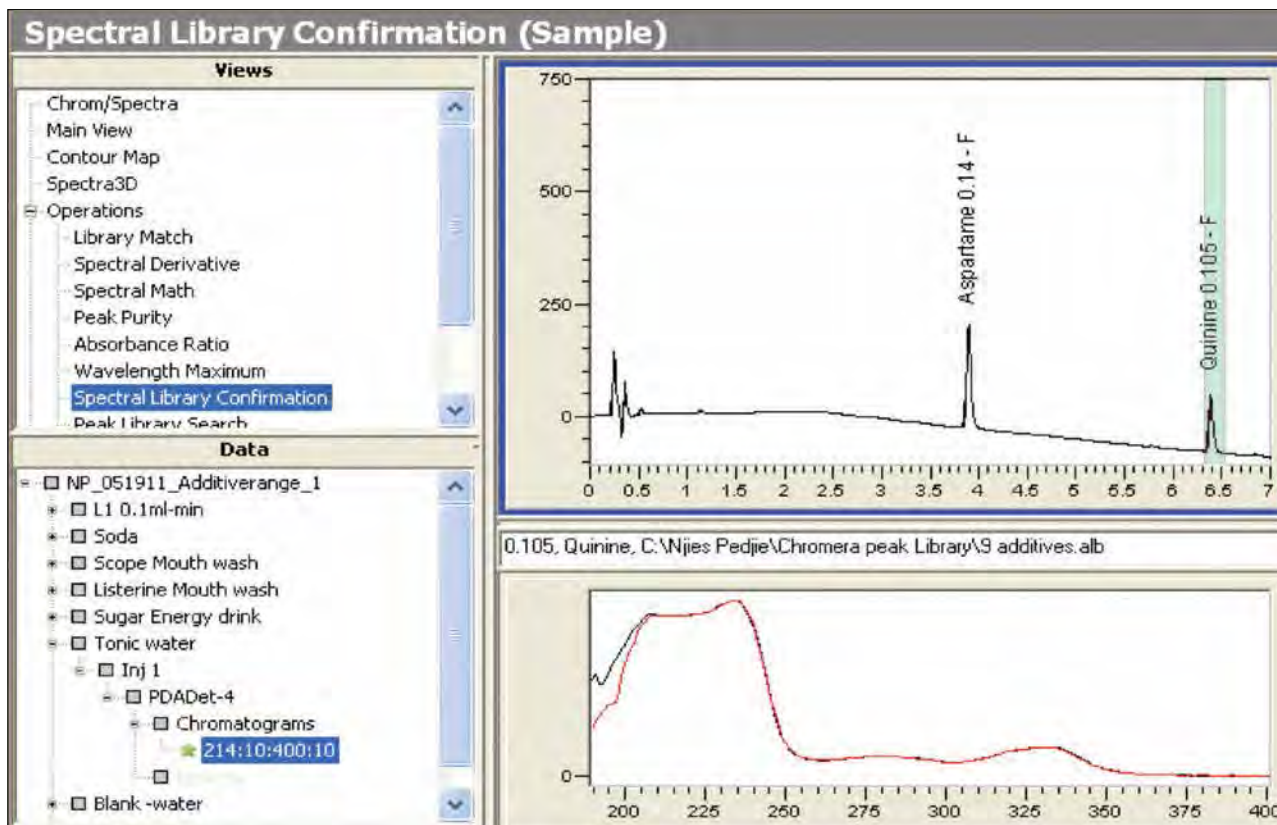


Figure 5. Peak identification in the tonic soda sample using Chromera spectral library.

Conclusion

The application of UHPLC to the analysis of nine additives resolves the nine components' peak within seven minutes. The method was shown to be linear with $r^2 \geq 0.997$, precise with $\%RSD \leq 1.33$; and accurate with an average recovery of 97.1%. The mouthwash tested is sweetened with 151 mg/12 oz saccharine and has 178 mg/12 oz of benzoic acid. The tonic soda is sweetened with 117 mg/12 oz of aspartame and has 69 mg/12 oz of benzoic acid. PerkinElmer's Flexar FX PDA detector provides rugged and accurate detection over a range of 190 nm to 700 nm, encompassing UV and visible wavelengths. PerkinElmer's Chromera software offers many data acquisition and processing features: spectral library creation, and peak purity, spectra 3-D and contour maps, which are powerful tools that give insight to the information content of a 3-D photodiode array chromatogram. The spectra library search function allowed the storage of standard peaks spectra that were later used for peak identification confirmation in the samples.

References

1. American Diabetes Association, 2007 National Diabetes Facts; Standards of Medical Care in Diabetes, 2008; Diabetes Care. 2009; 32:S13-S61, 2009.
2. FDA, Generally Recognized As Safe (GRAS) 21 CFR 170.30(b), 170.30(c) and 170.3(f).
3. Food Ingredient and Colors IFIC and FDA, November 2004, revised 2010.
4. Leo M.L. Nollet. Food Analysis by HPLC. Marcel Dekker, NY, 2000, pp. 99, 546.

Note: This application is subject to change without prior notice.



UHPLC

Author

Njies Pedjie

PerkinElmer, Inc.
Shelton, CT USA

Analysis of Color Additives in Beverages with the PerkinElmer Flexar FX-15 System Equipped with a PDA Detector

Introduction

Food colors have a great impact on consumers' perception of food quality. That explains why the use of color additives or dyes in food has become pervasive, not only in highly processed food such as cereals and frozen dessert, but also in seemingly natural food such as dairy products. Dyes are used to intensify the color of food products and make them look tempting. They are also used

to minimize color variation, and to prolong color stability on shelf. There are instances however, where dyes are used unscrupulously to mask the poor quality of food products. In the U.S., the Food and Drug Administration's (FDA) data shows an alarming five-fold increase in consumption of dyes since 1955.

Color additives in food products have practically no nutritional value. Some color additives are of natural origin and are generally safe but most are synthesized from petroleum and have the potential of tainting food supplies. A commonly used dye in the U.S. called sunset yellow has carcinogenic impurities such as sudan I. In vitro studies suggest that brilliant blue, another widely used dye has the potential for neurotoxicity. A study by Schab (2004) and another study by McCann (2007) suggest that mixtures of dyes cause hyperactivity and other behavioral problems in some children. In 2010, acting on these concerns, European countries mandated a warning label stating that food containing dyes may have adverse effect on activity and attention in children.

All around the world, toxicological considerations are prompting regulatory agencies to lower the acceptable level of dyes in comestible products. These different regulations are continuously harmonized by the Food and Agriculture Organization (FAO) and the World Health Organization (WHO) in order to promote food safety and trade. In the U.S. certified synthetic colorings (FD&C colors) are regulated by the FDA. In Europe, their regulation is under the European Commission's directives governing food dyes. In all these countries there is a push by consumer protection agencies to ban their use altogether.

This application note presents a fast and robust HPLC method for the determination of dyes in beverages (Table 1). Method conditions and performance data including precision and linearity are presented. A popular orange soda is analyzed and the type and amount of dyes used are confirmed.

Table 1. Dyes analyzed.

Dyes name	U.S. Code	EU Code
Amaranth	FD&C Red # 2 ¹	E123
Indigo Carmine	FD&C Blue # 2	E132
Sunset Yellow	FD&C Yellow # 6	E110
New Coccine	Red # 18	E124
Eosin Y	Acid Red # 87	
Erythrosin B	FD&C Red # 3	E127
Phloxine B	Acid Red # 92	
Rose Bengal	Acid Red # 94	

¹ Banned in food in the USA.

Experimental

A 0.1 mg/mL stock standard solution was prepared by diluting the appropriate net weight of the eight dyes with methanol followed by 15 min. sonication. From the stock standard four calibration levels were prepared by dilution with water (Table 2). The calibration curve and the repeatability were evaluated with three injections per level. The solutions were thoroughly mixed and filtered with a 0.2 µm nylon membrane prior to testing. The orange soda was filtered and injected directly.

Table 2. Calibration preparation.

	Level 1	Level 2	Level 3	Level 4*
Stock Std. (mL)	2.5	1.25	0.6	–
Total Vol. (mL)	10	10	10	10
Conc. (µg/mL)	25	13	6	3

*Level 4 is a direct 1:1 dilution from level 3.

Table 3. Detailed UHPLC system and chromatographic conditions.

Autosampler:	Flexar™ FX UHPLC												
Setting:	50 µL loop, partial loop injection mode 350 µL mixer volume injection 4 µL; flush solvent: methanol												
PDA Detector:	Scanned from 190-700 nm, analytical wavelength 254 nm Reference 400 nm, bandwidth 10 nm												
HPLC Column:	PerkinElmer Brownlee™ analytical C-18, 150 x 4.6 mm, 5 µm at 55 °C (Cat. No. N9303513)												
Mobile Phase:	A: 20 mM ammonium acetate B: 80:20 acetonitrile:methanol												
	<table><tr><th>Time (min)</th><th>Flow rate (mL/min)</th><th>B %</th><th>Curve</th></tr><tr><td>8</td><td>1.2</td><td>5-60</td><td>1</td></tr><tr><td>2</td><td>1.2</td><td>60</td><td>1</td></tr></table>	Time (min)	Flow rate (mL/min)	B %	Curve	8	1.2	5-60	1	2	1.2	60	1
Time (min)	Flow rate (mL/min)	B %	Curve										
8	1.2	5-60	1										
2	1.2	60	1										
	Three minutes equilibration after injection.												
Software:	Chromera® version 3.0												
Sampling Rate:	5 pts/sec												

Results and Discussion

The separation was achieved using a PerkinElmer Brownlee analytical C-18, 5 µm, 150 x 4.6 mm column. The optimal flow rate was 1.2 mL/min and the run time was about ten minutes with a back pressure of approximately 3000 PSI (207 bar). All eight components were well resolved with resolution ranging from 2.7 to 9.4. The calibration curve demonstrates a coefficient of determination not less than the cutoff of 0.999. The repeatability was good with %RSD values ranging from 1.0 to 1.9 along the four levels of calibration. The tailing was excellent with value not more than 1.4 (cutoff value is 2.0). Representative chromatograms of the standard solutions are shown in Figures 1 and 2; a representative chromatogram of the orange soda analyzed is presented in Figure 3. In Figure 4 the color additive in the orange soda is confirmed using the spectral library. The calibration curve and the performance of the method are presented in Figure 5 and Table 4.

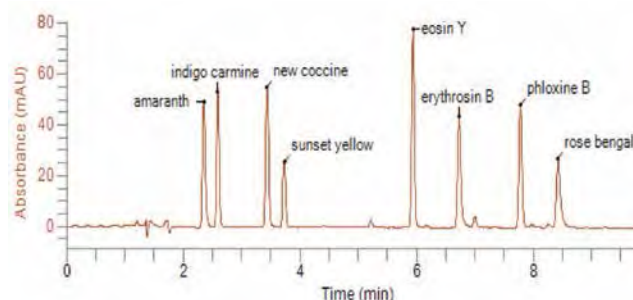


Figure 1. Chromatogram from the analysis of a 25 µg/mL standard solution.

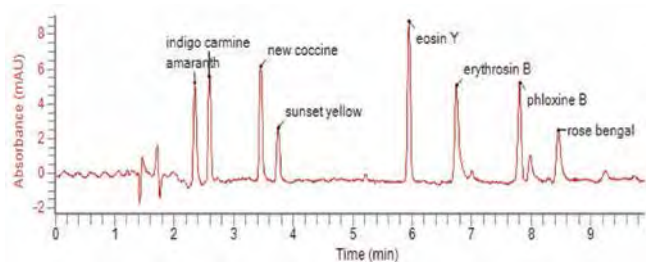


Figure 2. Chromatogram from the analysis of a 3 µg/mL standard solution.

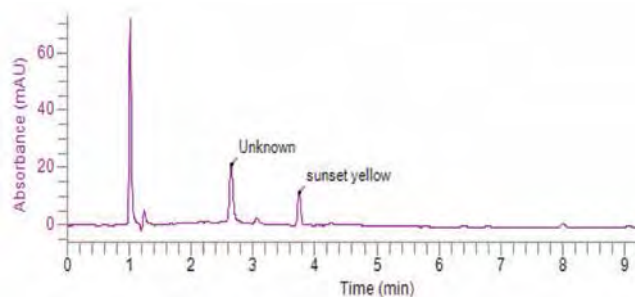


Figure 3. Chromatogram from the analysis of a popular orange soda.

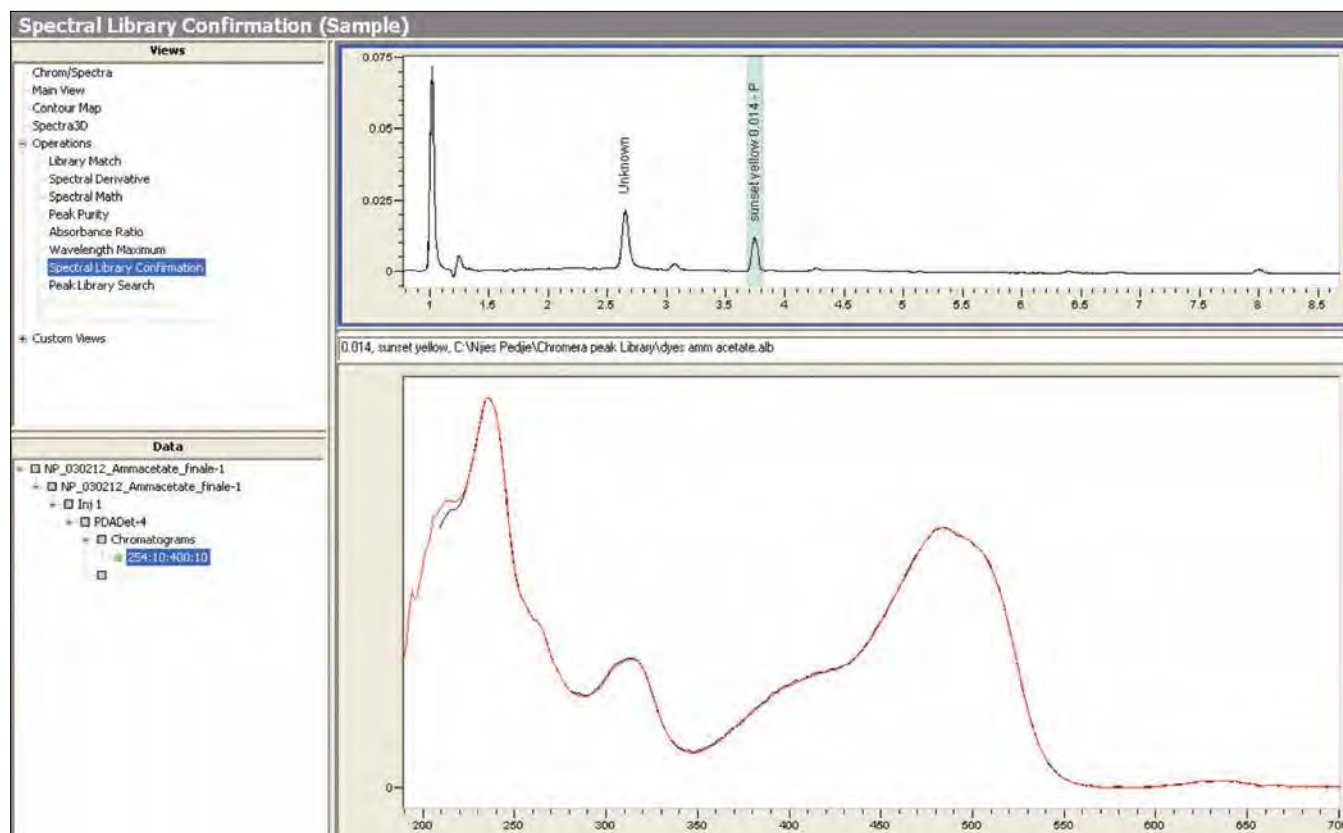


Figure 4. Peak identification in sample using Chromera spectral library

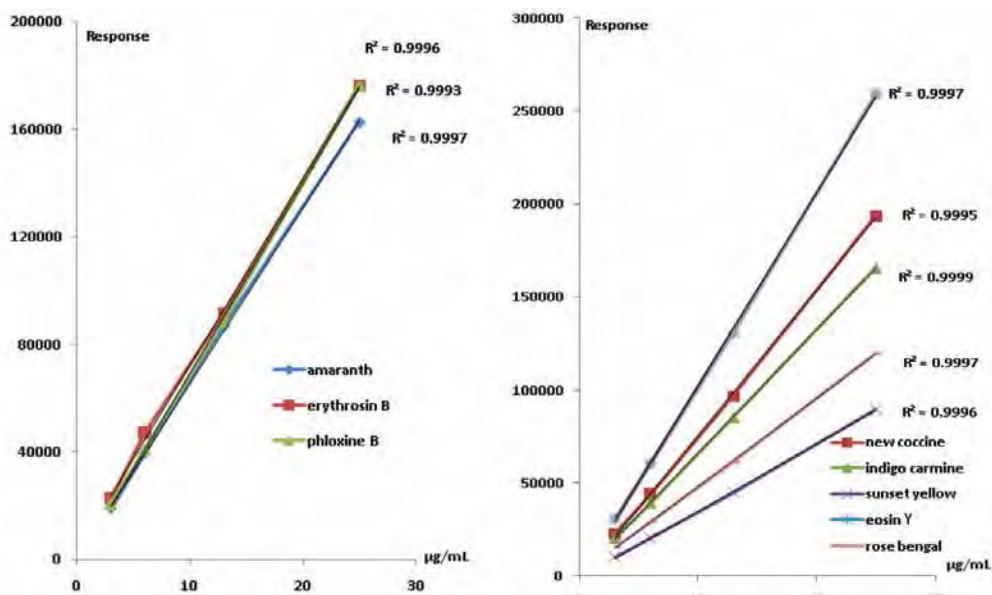


Figure 5. Calibration curves.

Table 4. Method performance.

Compound	Repeatability %RSD (n = 9)	Resolution	Tailing (n = 9)	Soda (µg/mL)
Amaranth	1.2	–	1.4	ND
Indigo Carmine	1.1	2.7	1.2	ND
New Coccine	1.1	9.4	1.2	ND
Sunset Yellow	1.6	3.1	1.1	11.0
Eosin Y	1.4	8.2	1.1	ND
Erythrosin B	1.0	7.9	1.4	ND
Phloxine B	1.7	8.6	1.1	ND
Rose Bengal	1.9	3.8	1.3	ND
Average	1.4	6.2	1.3	

Conclusion

Increased awareness of food safety is driving the improvement in quality control methodologies. In a world where global sourcing of food products is becoming the norm, concern about the type and quantity of color additives in food products is prompting regulators to harmonize regulations worldwide and is forcing the food industry to adopt stringent requirements. The method in this study, with outstanding performance and a calibration curve encompassing the concentrations at which dyes are typically used, subscribes to that effort. All the eight color additives analyzed were resolved within ten min. with resolution between consecutive peaks not less than the cutoff value of 1.5. The method was shown to be precise and linear with %RSD less than 2%, and r^2 not less than 0.999. The popular orange soda analyzed has 11.0 µg/mL of sunset yellow, far less than the 20 µg/mL maximum amount allowed in drinks in the European countries.

PerkinElmer's Flexar FX 15 pump fitted with durable pistons is capable of generating at each stroke a pressure up to 18000 PSI. A low dispersion injection valve combined with a carefully designed mixer capable of delivering a very precise and constant gradient result in very reproducible peaks

during analysis. The wide flow range capability (0.01 - 5.0 mL/min.) allows the use of a traditional HPLC column as well as columns specifically designed for UHPLC. The low dispersion PDA detector provides a rugged and accurate detection over a range of 190 nm to 700 nm wavelengths. PerkinElmer's Chromera software offers many data acquisition and processing features: spectral library creation, peak purity, spectra 3D and contour maps. Among these features, the spectral library function showcased in this application note is a powerful tool used to confirm the identity of components in the sample. It adds certainty to the results as it is known that components with the same relative retention time are not necessarily the same.

References

1. "Dyes, ADHD and Behavior: A Quarter Century Review – 2009 Update." Jacobson M, Schart D. (Washington Center for Science in the Public Interest). <http://cspinet.org/new/pdf/dyesreschbk.pdf>; retrieved Jan. 19, 2012.
2. McCann D, Barrett A, Cooper A, November 2007. Food Additives and Hyperactive Behavior in 3-year-old and 8/9-year-Old Children. The Lancet, Vol 370, pages 1560 - 1567.
3. Schab D, Trinh N., December 2004. Do Artificial Food Colors Promote Hyperactivity in Children with Hyperactive Syndromes? J. Dev. Behav. Pediatr. Vol 25, pages 423 - 434.
4. FDA: Food Ingredients and Colors. Revised in April 2010. <http://www.fda.gov/food/foodingredientspackaging/ucm094211.htm>; retrieved March 16, 2012.
5. European Commission. Food Safety: Food Additives. http://ec.europa.eu/food/fs/sfp/flav_index_en.html (contains links to relevant legislation).
6. Food Dyes A Rainbow of Risks. Center for Science in the Public Interest cspinet.org/new/pdf/food-dyes-rainbow-of-risks; retrieved Jan. 19, 2012.

Note: this application note is subject to change without prior notice.

Liquid Chromatography

Author

Njies Pedjie

PerkinElmer, Inc.
Shelton, CT 06484 USA

Analysis of Common Sweeteners and Additives in Beverages with the PerkinElmer Flexar FX-15 System Equipped with a PDA Detector

Introduction

Sweeteners are low or zero-calorie sugar substitutes that are added in drinks, processed foods and pharmaceutical products to provide the sweet taste of table sugar, which is also called sucrose. Sweeteners, especially artificial sweeteners, contain practically no calories because their metabolism follows a different pathway than that of sucrose. On the other hand, the intake of sucrose and the calories that derive from its metabolism is one of the leading causes of obesity and its related health problems including heart disease and diabetes.

People with diabetes are unable to properly metabolize sucrose causing an abnormally high concentration of it in the blood stream with damaging effects on blood vessels and other vital body organs. In 2007 there were 23.6 million people in the U.S. living with diabetes with an alarming 1.6 million new cases each year at an annual cost of \$174 billion. Worldwide, about 246 million people live with diabetes, with another seven million more cases each year making it a global epidemic. Substituting sucrose with artificial sweeteners, in addition to getting regular physical exercise and having healthy eating habits, is effective in fighting obesity and preventing or managing diabetes.

The use of artificial sweeteners is regulated in most countries. In the U.S., artificial sweeteners are part of the Generally Recognized As Safe (GRAS) ingredients. However, the FDA has established an Acceptable Daily Intake (ADI) for all sweeteners. Therefore manufacturers are required to list the type and amount of sweeteners on a food label. This application note presents a fast and robust liquid chromatography method to test widely used artificial sweeteners such as acesulfame potassium, saccharine and aspartame. A common stimulant and a preservative, namely caffeine and potassium benzoate were tested as well. The method was developed using a 3 μ m LC column to achieve very high throughput at a low flow rate to reduce the testing time and solvent usage. The throughput was compared to that of a conventional HPLC analysis with a 5 μ m particle column. In addition to throughput comparisons, method conditions and performance data including precision and linearity are presented. The results of the method applied to two popular soft drinks and two popular coffee sweeteners are reported.

Experimental

A working standard solution containing 200 μ g/mL of acesulfame potassium, potassium benzoate, aspartame, and 100 μ g/mL of saccharine and caffeine was prepared by dissolving neat material in water.

Repeatability was studied with six injections of the working standard. Linearity was determined across the range of 2-200 μ g/mL concentration. About 0.5 g/mL of two cola drinks from two major competitive brands were prepared by dilution with water. About of 2 mg/mL of two popular sugar substitutes were prepared individually by dissolving the sample in water followed by two min. vortexing. The solutions were thoroughly mixed and filtered with a 0.2 μ m nylon membrane prior to testing.

A PerkinElmer® Flexar® FX-15 UHPLC system fitted with a Flexar FX PDA photodiode array detector was used. The separation was achieved using a Restek® Pinnacle® DB C18, 3 μ m, 100 x 2.1 mm column. The run time was 3.5 min with a back pressure of 6050 PSI (417 bar).

Table 1. Detailed UHPLC system and chromatographic conditions.

Autosampler:	Flexar FX UHPLC
Setting:	50 µL loop and 15 µL needle volume, partial loop mode
Injection:	4 µL for UHPLC column, 10 µL for HPLC column
Detector:	Flexar FX PDA UHPLC Detector
Analytical Wavelength:	214 nm
Pump:	Flexar FX-15 UHPLC Pump
UHPLC Column:	Restek® Pinnacle® DB C18, 3 µm, 100 x 2.1 mm (Cat # 9414312)
HPLC Column:	PerkinElmer Brownlee™ Analytical C-18, 5 µm, 250 x 4.6 mm (Cat #N9303514)
Column Temperature:	Ambient, 30 °C
Mobile Phase:	A: 0.1% TFA in water B: 0.1% TFA in acetonitrile (HPLC grade solvent and ACS grade reagent)

Conventional C18 HPLC column			
Time (min)	Flow rate (mL/min)	B %	Curve
6	1.0	10-35	1
4	1.0	70	1
2	1.0	70	1

UHPLC C18 column			
Time (min)	Flow rate (mL/min)	B %	Curve
3.5	0.7	5-40	1

Sampling Rate:	5 pt/s
Software:	Chromera Version 3.0

Results And Discussion

Initially, the method was developed with a conventional C18, 250 x 4.6 mm, 5 μ m particle size HPLC column. The optimal flow rate of this method was determined to be 1.0 mL/min. at ambient temperature. All the peaks eluted within 12 min. (see Figure 1). By using a shorter column with smaller particle size (C18 100 x 2.1 mm, 3 μ m particle size) suitable for UHPLC, the run time was dramatically reduced from 12 min. to about 3.5 min. at 30 °C (see Figure 2).

In addition to the more than threefold reduction in chromatographic run time, the flow rate was reduced to 0.7 mL/min. from 1.0 mL/min. Thus, 70% reduction in testing time and 80% reduction in solvent usage was achieved by moving to the UHPLC method. This is important not only because of the relatively high cost of HPLC-grade solvents, but also because far less solvent must be disposed of as waste. This results in a much lower cost of ownership and a much greener lab operation.

Excellent method performance was achieved. The linearity of the analysis achieved a R-squared value of at least 0.999 for each additive tested and precisions values ranged from 0.9 - 1.5% RSD. Details of the method performance and results of the sample tested are presented in Table 2 and Table 3.

Table 2. Precision and linearity.

	Acesulfame K	Saccharine	Caffeine	Aspartame	Potassium benzoate
%RSD (n=6)	0.9	1.5	1.3	1.3	1.0
r ²	0.9997	0.9995	0.9993	0.9993	0.9999
Range (µg/mL)	4-200	2-100	2-100	4-200	4-200

Table 3. Amount of additives in samples.

Compound	Cola Drink 1 (mg/12 oz)	Cola Drink 2 (mg/12 oz)	Sweetener 1 (mg/g)	Sweetener 2 (mg/g)
Acesulfame K	ND	ND	ND	ND
Saccharine	ND	ND	ND	30
Caffeine	47	35	ND	ND
Aspartame	181	157	40	ND
Potassium benzoate	71	74	ND	ND
<i>ND = None detected</i>				

A spectrum of each component was obtained from the analysis of the standard solution over a range of 190 nm to 700 nm, and the wavelength maximum was determined, enabling the selection of a suitable wavelength setting for the analysis.

PerkinElmer's Chromera® software helps in assessing the purity of each peak by comparing the spectra on the upslope and the down slope of the peak. Because a pure peak has matching spectra throughout the peak, a ratio of upslope/down slope absorbance greater than 1.5 could be an indication of a co-elution. The spectrum and the purity of one of the sweeteners tested are presented in Figure 3.

Although in liquid chromatography peak identification is usually based on the retention time, Chromera's ability to collect and store spectra offers another way of identification by matching any peak spectrum to spectra stored in its library. This feature of Chromera adds another level of confidence in the analysis as the same relative retention time does not necessarily mean the components are the same. Confirmation of the presence of caffeine, aspartame and potassium benzoate in the Cola Drink 1 sample is shown in Figure 4. In that figure, the spectra at the peak apex of each peak is compared with the spectra of the standard stored in the library. When a match is made, the name of the matching spectrum appears on each peak in question, confirming its identity.

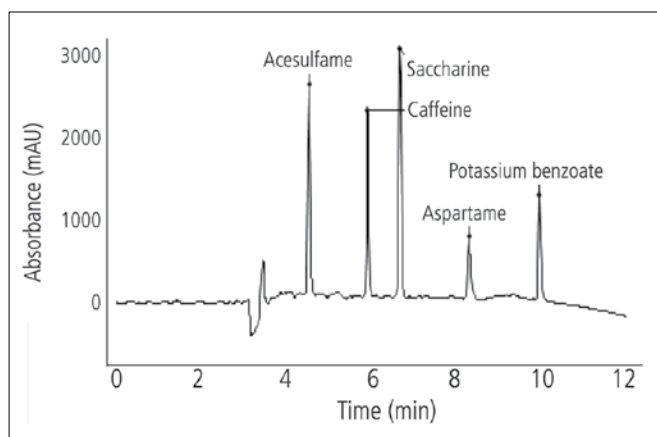


Figure 1. Chromatogram from the analysis of a standard with conventional HPLC C18 250 x 4.6 mm, 5 µm column.

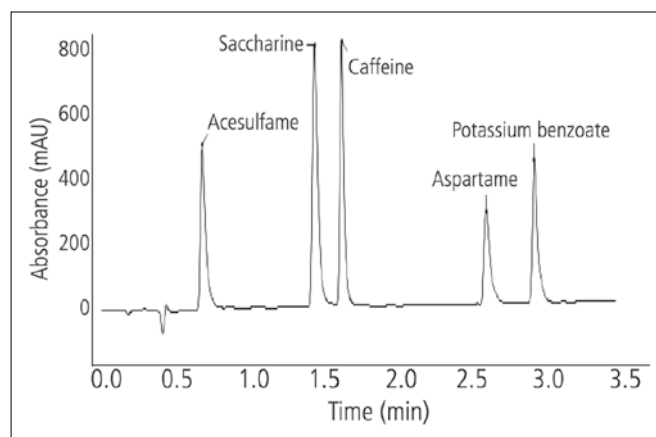


Figure 2. Chromatogram from the analysis of a standard UHPLC C18 100 x 2.1 mm, 3 µm column.

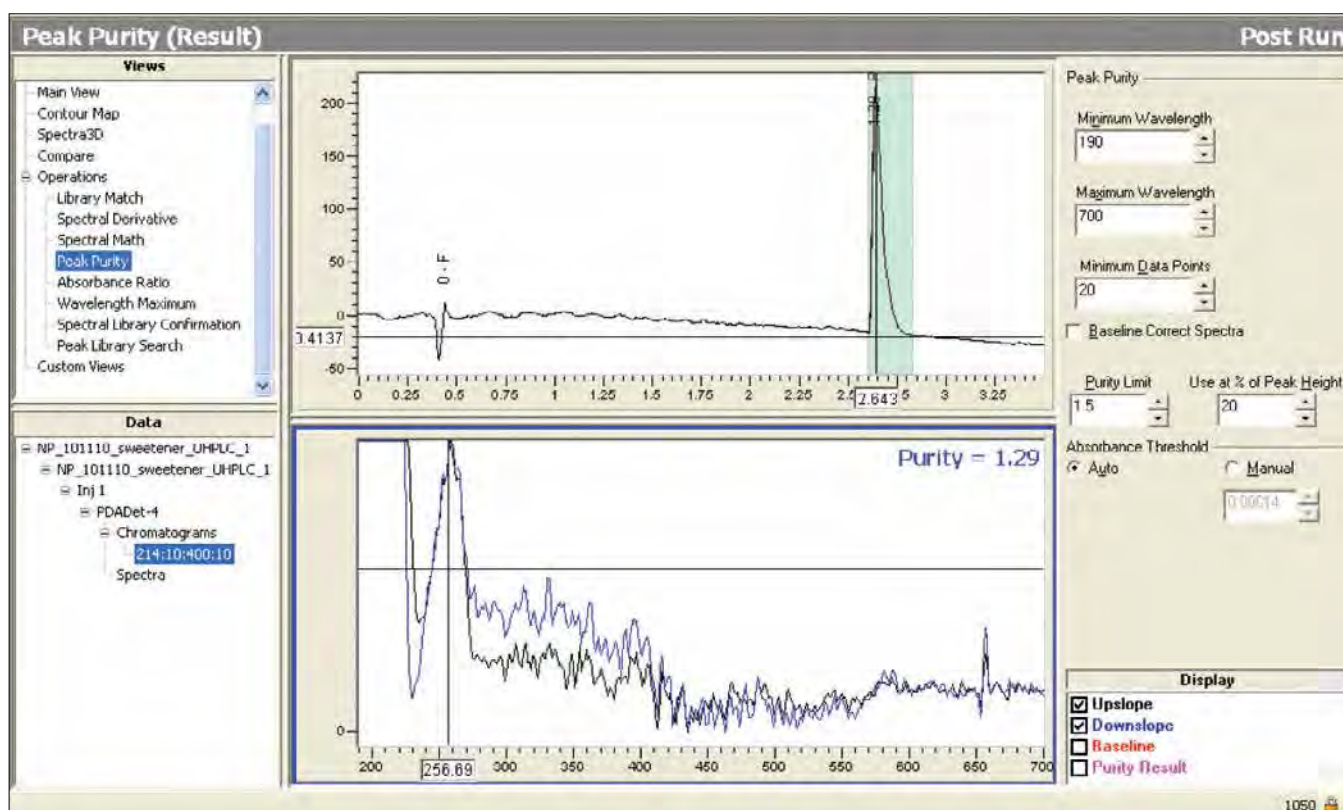


Figure 3. Chromatogram of the analysis of Sweetener 1 and the assessment of the peak purity.

Conclusion

The application of UHPLC to the analysis of artificial sweeteners and soft drink additives resulted in 70% reduction in run time, as well as 80% reduction in solvent usage. The PerkinElmer Flexar FX-15 UHPLC system and Restek® Pinnacle® DB C18, 3 µm, 100 x 2.1 mm resolved all five additives studied in about three and half minutes.

The method was shown to be linear and the peaks were well resolved. Both of the soft drinks tested were sweetened with aspartame: 181 mg/12 oz for Cola Drink 1 and 157 mg/12 oz for Cola Drink 2. The level of caffeine in drinks was similar to the label claim of 45 mg/12 oz for Cola Drink 1 and 35 mg/12 oz for Cola Drink 2. Both of the drinks have similar amounts of potassium benzoate: 71 mg/12 oz for Cola Drink 1 and 74 mg/12 oz for Cola Drink 2. The PerkinElmer

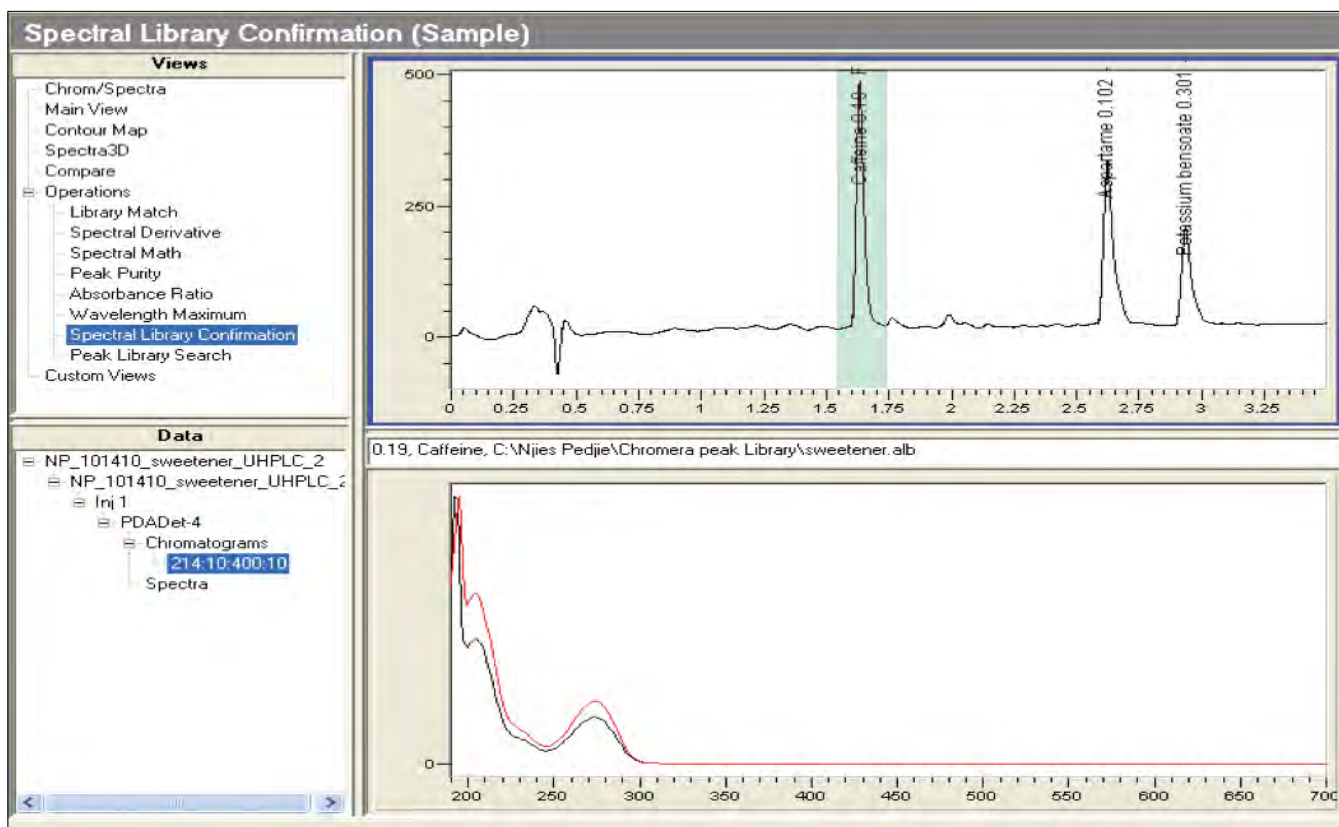


Figure 4. Chromatogram of the Cola Drink 1 and spectra library confirmation.

FX PDA detector provides rugged and accurate detection over a range of 190 nm to 700 nm, encompassing UV and visible wavelengths. PerkinElmer's Chromera software offers many data acquisition and processing features: spectral library creation, and peak purity, spectra 3D and contour maps, which are powerful tools for interrogating the information content of a 3D photodiode array chromatogram. The spectra library search function allowed the storage of standard peaks spectra that were later used for peak identification confirmation in the sample.

References

1. American Diabetes Association. 2007 National Diabetes Facts; Standards of Medical Care in Diabetes – 2008; Diabetes Care. 2009; 32:S13-S61, 2009.
2. FDA, Generally Recognized As Safe (GRAS) 21 CFR 170.30(b), 170.30(c) and 170.3(f).
3. Leo M.L. Nollet. Food Analysis by HPLC. Marcel Dekker, NY, 2000, pp. 523-565.
4. Food Ingredient and Colors, IFIC and FDA, November 2004, revised 2010.
5. International Diabetes Federation, Diabetes Epidemic Facts.

Dissolution of Gelatin Monitored by DMA



Summary

This application note describes the dissolution process of gelatin obtained from an empty pharmaceutical gelcap using a PerkinElmer® DMA 8000. The experiment was performed by cutting a piece of gelatin from the gelcap and mounting it in the DMA 8000. The sample was immersed in water and the mechanical properties monitored as a function of time.

It will be shown how the temperature greatly influenced dissolution rate. The modulus gives a good indication of the softening of the material over time and the $\tan \delta$ gives an indication of the material becoming more viscous over time.

Introduction

Gelatin is commonly used in both foods and pharmaceuticals. Pharmaceutically, a gelcap is used to encapsulate an active ingredient or therapeutic formulation. The composition of the gelatin can be formulated to give the best dissolution profile with respect to pH, temperature etc. so that the contents are released at the appropriate time after swallowing. The thickness, overall size, shape and composition of the gelcap can all influence the dissolution properties.

DMA works by applying an oscillating force to the material and the resultant displacement of the sample is measured. From this, the stiffness can be determined and modulus and $\tan \delta$ can be calculated. $\tan \delta$ is the ratio of the loss modulus to the storage modulus. By measuring the phase lag in the displacement compared to the applied force it is possible to determine the damping properties of the material. $\tan \delta$ is plotted against temperature and glass transition is normally observed as a peak since the material will absorb energy as it passes through the glass transition.

This application note will describe some experiments where a sample of gelatin is immersed in water at different temperatures. One advantage of the DMA 8000 is the ability to immerse samples in any geometry. The mechanical properties of the sample as dissolution commences will be discussed and comparison of the different temperature data will be discussed.

Experimental

Isothermal immersion study of gelatin.

An empty gelcap was cut up to provide small strips of gelatin which were mounted in the DMA 8000. The samples were immersed in water and the $\tan \delta$ and modulus were monitored as a function of time. The experiment was repeated at a second temperature.

Equipment	Experimental Conditions	
DMA 8000 Fluid Bath Circulator	Sample:	Empty Gelcap
	Geometry:	Single Cantilever Bending
	Dimensions:	3.2 (l) x 5.0 (w) x 0.7 (t) mm
	Temperature:	25 °C and 38 °C isothermally
	Frequency:	1.0 Hz

Results and conclusion

Figure 1 shows the response from the DMA as a function of time. The time data is adjusted so the point of immersion is shown as 30 seconds after the start of the experiment.

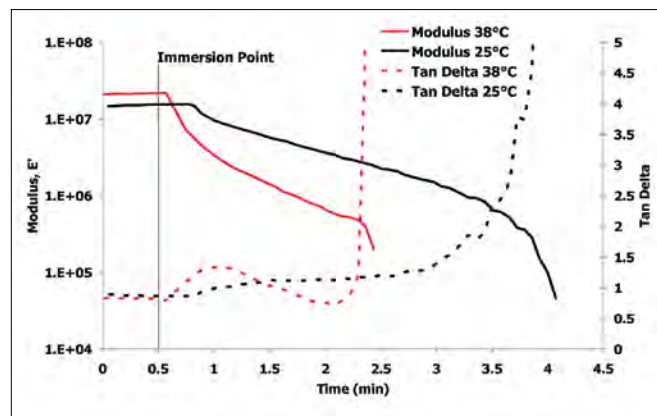


Figure 1. DMA data from immersed gelcap.

In both samples, the modulus decreases with time after immersion reflecting the sample getting less stiff as it dissolves. Eventually, the sample disintegrates so much that data is meaningless and this is the point where the data collection was ceased. The sharp decrease in modulus indicates this point. It is worth noting that the rate of softening and the time taken to destroy the sample were both faster at 38 °C than 25 °C. Also, the initial ingress of water into the gelatin to start the dissolution process was much faster at 38 °C as shown by the short time between immersion and modulus decrease starting.

The $\tan \delta$ data is often referred to as the damping factor and can indicate the sample becoming less elastic and more viscous if $\tan \delta$ increases. The end point of both experiments show this behavior as expected. The sample is no longer a self supporting solid but rather a viscous semi-solid which would display more viscous characteristics. The 38 °C data, and to a lesser extent the 25 °C data, shows a broad peak which might indicate a swelling of the material as a prelude to dissolution.

It has been demonstrated how the DMA 8000 can investigate dissolution and swelling behavior of materials by utilizing the immersion function of the fluid bath. Valuable mechanical information was generated from gelatin using this approach. Testing in solution will often give information not available from running samples in air.

Increased Throughput and Reduced Solvent Consumption for the Determination of Isoflavones by UHPLC

Authors:

Padmaja Prabhu, PerkinElmer
Wilhad Reuter, PerkinElmer

Liquid Chromatography



Studies suggest that the isoflavones found in soy can exert positive physiological effects.

Introduction

All plant foods are complex mixtures of chemicals including both nutrients and biologically active non-nutrients, referred to as phytochemicals. Soy is known for having high concentrations of several physiologically-active phytochemicals, including isoflavones, phytate (inositol hexaphosphate), saponins, phytosterols and protease inhibitors. The isoflavones are what makes soy unique. Soy isoflavones are non-steroidal molecules structurally and functionally related to 17β -estradiol. Soybeans and soy foods are the only natural dietary sources that provide nutritionally relevant amounts of isoflavones.

Clinical studies suggest that consumption of isoflavones can exert positive physiological effects¹. Recent data has demonstrated that isoflavones have potent antioxidant properties, comparable to that of the well known antioxidant vitamin E². Research in several areas of healthcare has linked isoflavones to lowering risks for disease, easing menopause symptoms, reducing heart disease and cancer risk, and improving prostate and bone health. As a result of the potential health benefits of isoflavones, many soy products and isoflavone supplements are available to consumers. These fall into a category of products known as nutraceuticals or functional foods, which provide a potential health benefit from a naturally occurring substance. This has created the need for an analytical technique which can qualify and quantify the type and amount of isoflavones in a nutraceutical product.

This application note will demonstrate a rapid method for the identification and quantification soy isoflavones using ultra high performance liquid chromatography (UHPLC). This UHPLC method is nearly 10x faster, and saves 92% of the mobile phase solvent, compared to conventional HPLC methods.

The focus will be on three major isoflavones found in soybeans, genistein, daidzein, and glycitein, and their glycosidic conjugates (Figure 1). In addition to qualitative and quantitative analysis, we will compare the analytical time and solvent use of this UHPLC application with a similar technique using conventional HPLC. The savings in both time and solvent consumption will be discussed. Lastly, three commercial formulations of supplements will be analyzed and isoflavone identification and content determined.

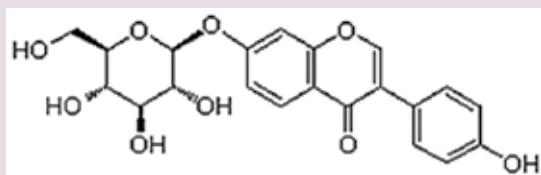
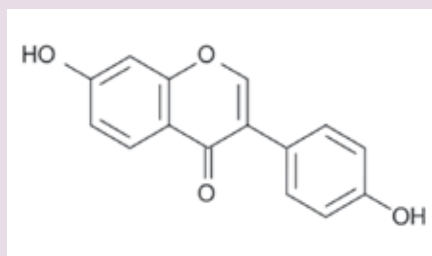


Figure 1. Chemical structure of a common soy isoflavone, daidzein, and its glycosidic conjugate, daidzin

Experimental

The PerkinElmer® Flexar™ FX-10 UHPLC system was used for this application. A 1.5 μ m particle, 50 mm length, C18 column was used to separate the analytes of interest and matrix. This column required an operating pressure of approximately 8500 psi resulting in a mobile phase flow rate of approximately 0.7 mL/min. A Flexar FX-UV/Vis UHPLC detector was operated at 254 nm. Table 1 presents the detailed operating parameters of the UHPLC system. The instrument interaction, data analysis, and reporting was completed with the PerkinElmer, Chromera® data system.

Table 1: Detailed instrument conditions used in the determination of isoflavones.

HPLC System	PerkinElmer Flexar FX-10 UHPLC
Autosampler	Flexar UHPLC Autosampler
Detector	Flexar FX UV/Vis UHPLC Detector
Column	Grace Vision HT C18 (50 mm x 1.5 μ , 2.1 mm i.d.)
Column Temperature	30 C
Detector Wavelength	254 nm
Injection Volume	2 μ L (partial loop)
Flow Rate	1 mL/min
Mobil Phase A	Water pH adjusted to 3.0 with orthophosphoric acid
Mobil Phase B	Acetonitrile Gradient Program

Type	Time (min)	Flow (mL/min)	% A	% B	Curve
Equil	0.5	0.7	90	10	0
Run	0.3	0.7	90	10	0
Run	0.3	0.7	85	15	0
Run	0.8	0.7	80	20	0
Run	0.9	0.7	75	25	0
Run	0.5	0.7	65	35	0
Run	0.5	0.7	90	10	0
Run	1.2	0.7	90	10	0

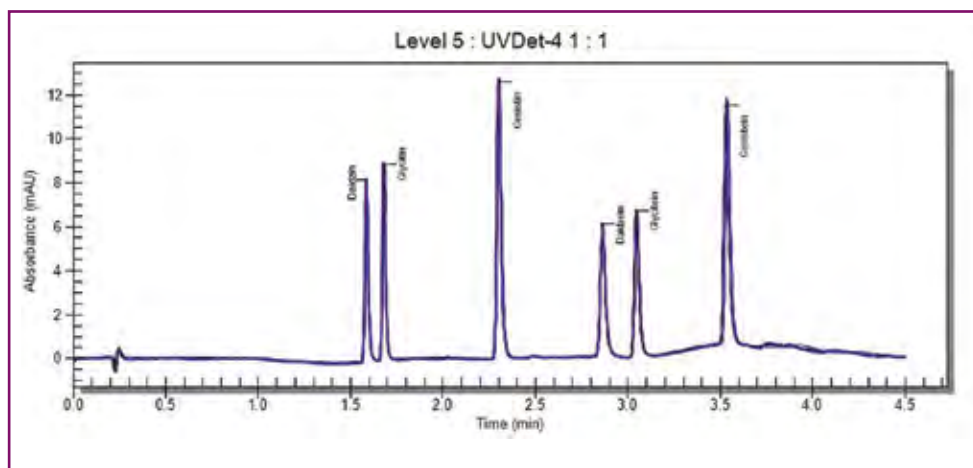


Figure 2. Resultant chromatograms of the analysis of reference material under the instrument conditions presented here (overlay of three replicates).

Standard preparation: The reference standards were procured from Chromadex (Irvine, CA).

Stock Solution: 1 mg of each of daidzin, glycitin, genistin, daidzein, glycitein and genistein were dissolved in 10 mL of water:acetonitrile (1:1), making a stock solution at a concentration of 100 µg/mL.

Calibration curve: The stock solution (100 µg/mL) was diluted in 9:1 (water:acetonitrile) to create an 8 level calibration (Table 2). The three low calibration points were serially diluted from the 10 µg/mL level, to reduce inaccuracies in the measurement to small volumes. The diluent in the calibration curve was used so that the solvent composition was as close as possible to the mobile phase composition at the time of injection. This will minimize baseline disturbance associated with injection. This is especially important in UHPLC where peak shapes can be distorted as a result of disturbance of the mobile phase composition.

Table 2: Scheme used for the creation of an eight level calibration.

Calibration Level	Concentration (µg/mL)	Volume of Standard Solution Added (mL)	Final Volume (mL)
1.	0.5	0.5*	10
2.	1	1*	10
3.	2	2*	10
4.	4	0.4	10
5.	6	0.6	10
6.	8	0.8	10
7.	10	1.0	10
8.	12	1.2	10

Calibration: The UV detector was calibrated across the range of 0.5 to 12 µg/mL, each calibration point was run in triplicate to demonstrate the precision of the system. The average coefficient of determination for a line of linear regression was 0.9965 for all 6 compounds. The calibration curves for daidzein and daidzin are pictured in Figure 3. Also in Figure 3 is the percent relative standard deviation (%RSD) for each calibration point (n=3). The precision of the system across the calibration range is excellent, the %RSD for diadzein and diadzin with an average of approximately 0.5%.

Sample preparation: Three commercially available supplements were analyzed with the method developed here. The samples are referred to as: sample 1, sample 2 and sample 3. The sample preparation used was relatively straightforward. A 0.5 gram sample of each supplement was ground with a mortar and pestle. The ground sample was extracted in 100 mL of (1:1) water: acetonitrile, in an ultrasonic bath. The sample extracts were filtered through a 0.2µm nylon filter. Following filtration, 2 mL of sample extract was diluted to 10 mL final volume in 9:1 (water:acetonitrile), this reduced the concentration of the isoflavones in the extract within the range of the calibration curve and made the diluents and mobile phase more alike.

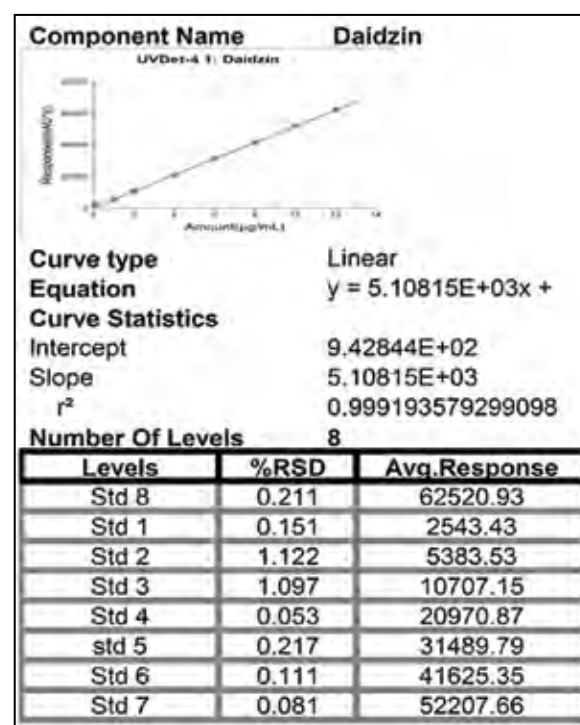
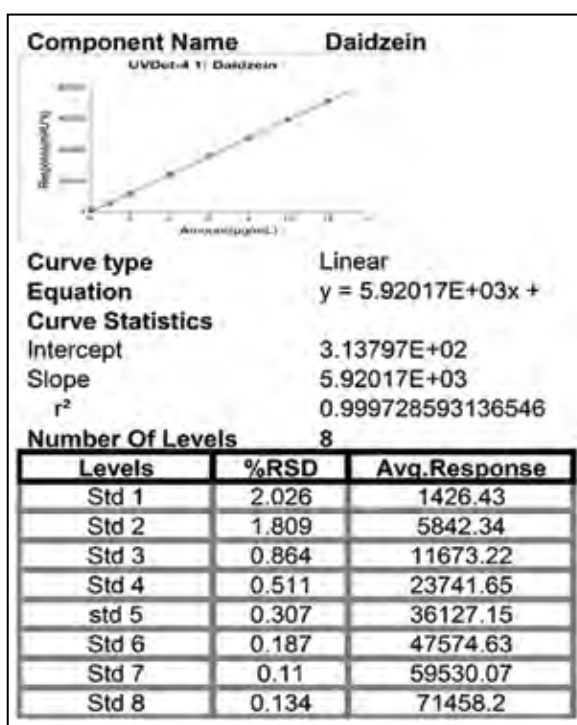


Figure 3. Example calibration results, via Chromera CDS.

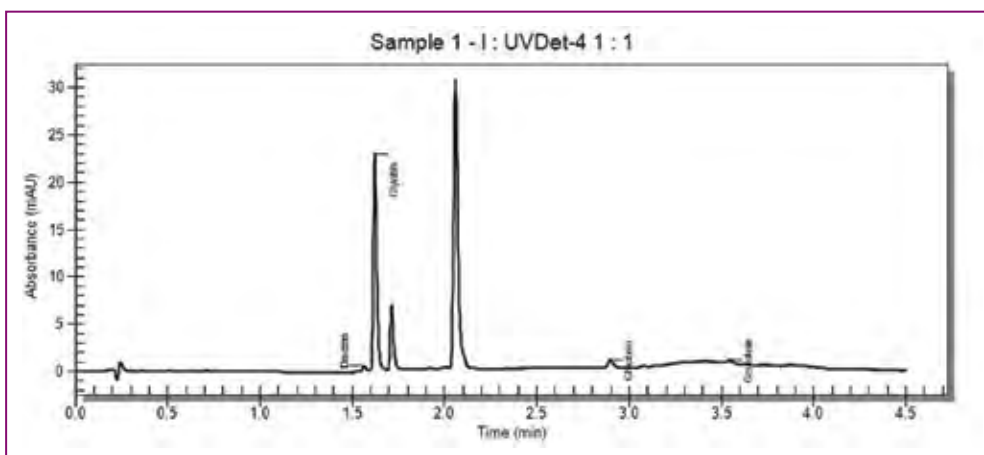


Figure 4: Example chromatogram of sample 1.

Results

Under the conditions presented here, the analytical run was 4.5 minutes long with an elution order of daidzin, glycitin, genistin, daidzein, glycitein and genistein. In similar applications performed with conventional HPLC, the analytical run time was 43 minutes. Therefore, this method has reduced the run time by 38.5 minutes, while maintaining complete resolution of all analyte peaks. The minimum resolution (critical pair) of analytes in this separation was 2.8, occurring between daidzin and glycitin.

The analysis of samples 1 and 2 resulted in detection of significant levels of isoflavones, with 49 and 52 mg of isoflavones in each sample, respectively. The label on the bottle for both samples 1 and 2 stated that each contained 55 mg of isoflavones per tablet, the determined values for each sample equate to 89% and 95% recovery. The sample analysis is summarized in Table 3. The analysis of sample 3 resulted in no detection of isoflavones; this was expected, as sample 3 was a multi-vitamin that did not list any isoflavones on its label.

Table 3. Summary of the results determined in the analysis of supplement samples for isoflavone content.

	Measured Isoflavone Content (mg)	Labeled Isoflavone Content (mg)	Percent Recovery
Sample 1	49	55	89%
Sample 2	52	55	95%
Sample 3	ND	0	n/a

Conclusions

The technique presented in this application note applies UHPLC instrumentation to the determination of isoflavones in nutraceutical supplements. A commercial reference standard was used to identify 3 isoflavones and their glycosidic conjugates by retention time. The separation used a short small particle (1.5 μm) LC column and achieved adequate resolution of all isoflavone peaks commonly found in soy materials. A multilevel calibration curve using the UV/Vis detector at 254 nm was used to quantitatively determine the amount of isoflavone in three dietary supplements. In addition to providing a precise and accurate result for the determination of isoflavones in supplements, this UHPLC application has reduced the analytical runtime by nearly 10x and eliminated nearly 40 mL of solvent use per sample. When compared to conventional HPLC, this directly translates into solvent savings of 92%.

References

1. www.soyconnection.com, IsoflavonesFactSheet.pdf
2. <http://www.isoflavones.info>



APPLICATION NOTE

Gas Chromatography/ Mass Spectrometry

Author

Andrew Tipler
Senior Scientist

PerkinElmer, Inc.
Shelton, CT USA

Using the D-Swafer to Investigate Solvent Impurities by Heartcutting GC/MS



Introduction

Solvents are widely used in the pharmaceutical and food industries for a variety of purposes. It is important that such solvents are carefully quality-control (QC) tested prior to use to ensure that no unsafe levels of impurities are present.

Gas chromatography (GC) is normally the preferred technique for the determination of impurities in solvents. The inclusion of a mass spectrometric (MS) detector enables the identities of the impurities to be established.

Because many solvents are produced by fractional distillation, their impurities will have similar boiling points to that of the solvent. Thus in GC, the retention times will be similar to that of the solvent and the risk of co-elution can be high.

Furthermore, if the MS is kept active during solvent elution, contamination of the ion source or analyzer may result, and the risk of filament damage is greatly increased. This application note describes a heartcutting technique that allows the entire injected sample to reach the detector and yet resolve the issues with solvent-peak resolution and potential detector damage.



Method

For this work, a D-Swafer™ Dean's Switch was configured as shown in Figure 1. This is a classic Dean's switch configuration, enabling cuts to be directed from the effluent of the first column into the inlet of the second column.

Tables 1 and 2 give further details of the analytical system and conditions applied.

The Swafer Setup Utility software, which is included with the product, was used to determine the geometry of the restrictor tubing connected to the FID. This is necessary to balance the flow rate in the secondary column in order for the Swafer switching to function correctly.

Table 1. Gas chromatograph configuration.

Component	Description
Gas Chromatograph	Clarus® GC
Heartcutting Device	D-Swafer in D4 configuration
Injector	Split/splitless
Detector 1	Flame ionization
Detector 2	Clarus GC/MS
Column 1	15 m x 0.25 mm x 1.0 µm Elite-1
Column 2	30 m x 0.25 mm x 1.0 µm Elite Wax
Restrictor	58 cm x 0.10 mm deactivated fused silica

Table 2. Analytical conditions.

	Setting	Value
Oven	Temperature	60 °C isothermal for 8 min
Carrier Gas		Helium
Injector	Temperature	225 °C
	Carrier-Gas Pressure (P1)	23 psig (159 kPa)
	Split Flow	100 mL/min
Midpoint	Pressure (P2)	16 psig (110 kPa)
Detector 1 (FID)	Temperature	250 °C
	Air Flow Rate	450 mL/min
	Hydrogen Flow Rate	45 mL/min
	Range	x20
	Attenuation	x64
Detector 2 (MS)	Temperature	200 °C
	Mass Range	15 to 150 Da
	Scan Time	0.2 sec
	Interscan Delay	0.1 sec
Sample Injection		1 µL by Autosampler in Fast Mode
Swafer Switching Valve (V4) Timed Events		See Results section

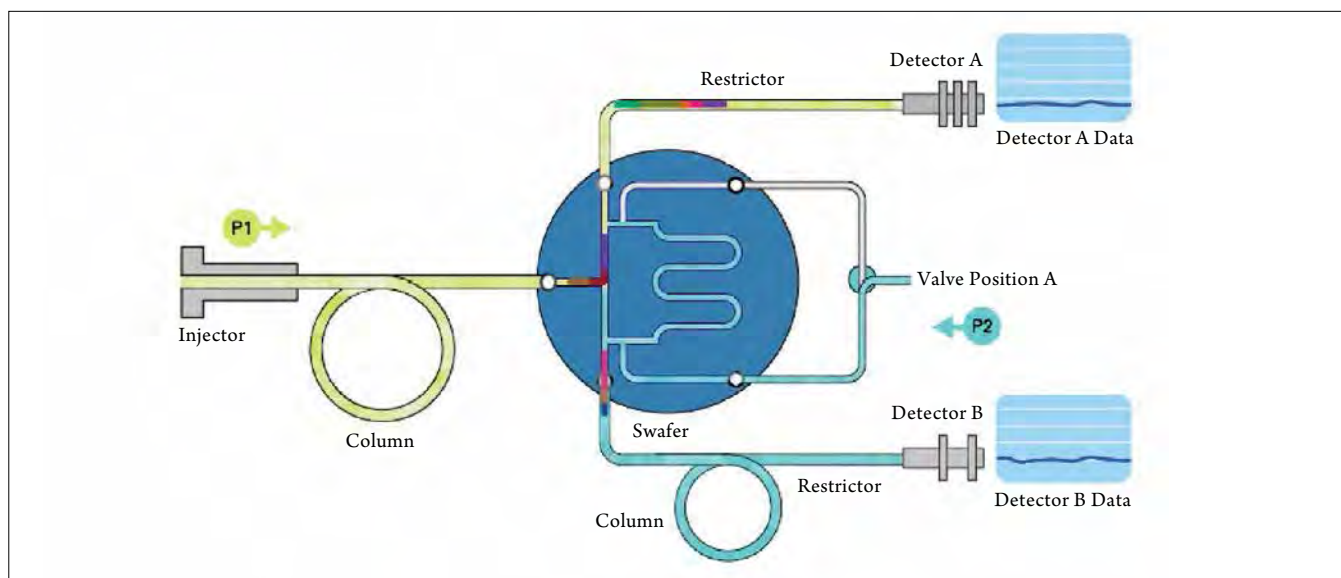


Figure 1. The D-Swafer in the D4 configuration for classic heartcutting.

Samples

For this work, 5 samples of analytical-grade dichloromethane (DCM) from different suppliers and a single sample of ethyl acetate were analyzed.

Results

With the Swafer switching solenoid valve (V4) turned off, the effluent from Column 1 was directed to Detector 1 – the flame ionization detector (FID). Figure 2 shows the chromatography observed on the FID from one of the DCM samples.

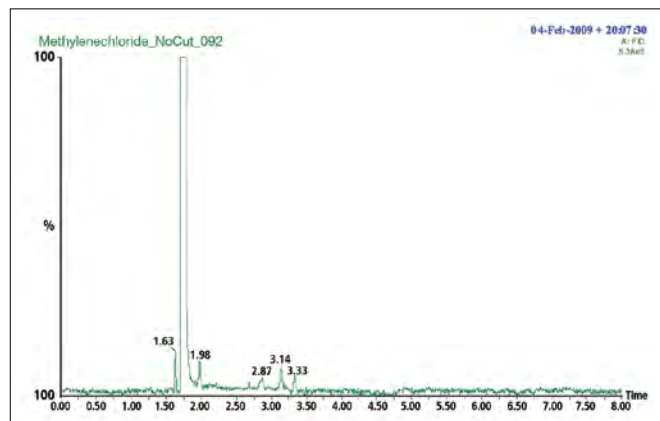


Figure 2. Chromatogram on Detector 1 (FID) of DCM sample 3, showing small impurity peaks.

With the relatively high split flow being applied, the FID will not provide very good detection limits for the impurities. Figure 2 shows a number of impurities around the main DCM peak that are only just above the background noise level. In practice, this will not be a limitation because the superior sensitivity of the MS system will allow much better detection limits to be obtained when these impurities are cut to the second column.

To check that the D-Swafer was working correctly, the signal was monitored on the MS detector while the chromatography was directed to the FID. Figure 3 shows that none of the sample reached the MS detector while the D-Swafer was switched to the other channel.

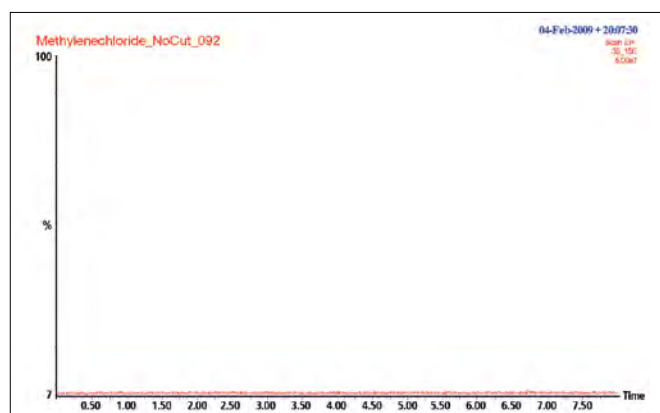


Figure 3. Signal seen on the MS while the D-Swafer is switched to the FID.

When V4 was switched on for the whole run, all effluent from Column 1 will be directed to the inlet of Column 2 and so the chromatography will occur in both columns and will appear at Detector 2 – the MS. Figure 4 shows the total ion chromatogram for DCM sample 3. Note the much better sensitivity to the impurity compounds than from the FID.

In Figure 4, we see the solvent peak dominates the chromatography around it and probably obscures some smaller peaks.

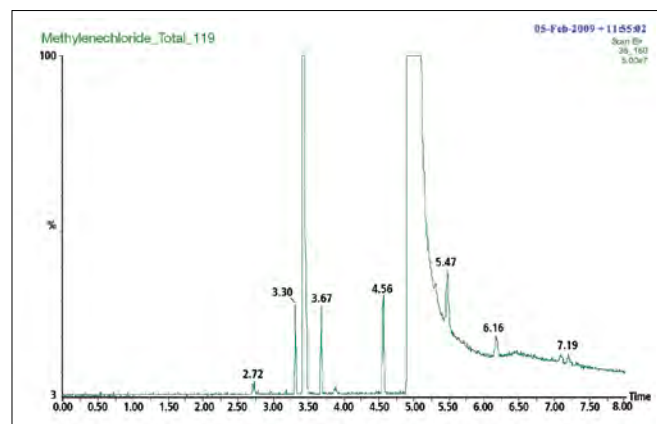


Figure 4. Total ion chromatogram on Detector 2 (MS) of DCM sample 3.

A run was made with V4 turned on at the start of the run and switched on during the solvent-peak elution on Column 1 and then switched off again. This sidecutting technique has the effect of removing a large fraction of the solvent, yet allowing the rest of the sample to enter Column 2. Figure 5 shows a chromatogram run this way.

Inspection of Figure 5 shows that much of the solvent has been removed by the sidecutting method. This removal is better illustrated by Figure 6 (Page 4), which shows the two chromatograms at a larger scale. Thus, sidecutting is a highly effective technique to keep solvent away from the MS detector.

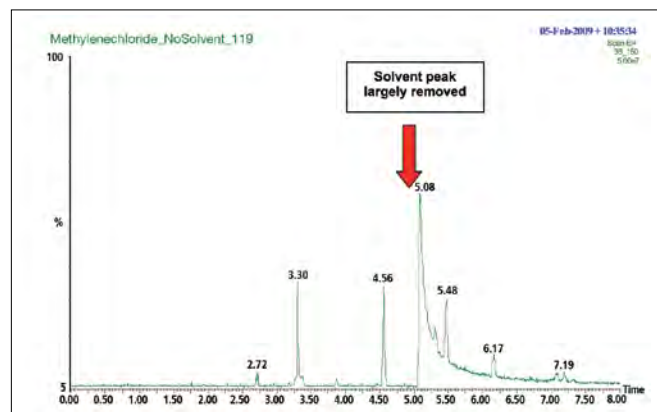


Figure 5. Total ion chromatogram on Detector 2 (MS), with solvent peak removed, of DCM sample 3. The switching valve was turned off between 1.68 and 1.80 minutes (refer to Figure 2 for context) but was on for the rest of the run.

Table 3. Tentative MS assignment of compound identities in DCM samples using the solvent sidecutting and heartcut sectioning technique.

Retention Time (min)	MS Identification	DCM Sample					
		1	2	3	4	5	
3.30	2-Methylbutane			√			
3.41+	Branched Chain Pentene*	√		√	√	√	
3.68+	Dichloroethylene*	√	√	√	√	√	
3.75	Branched Chain Hexane*				√		
3.87	Acetone	√		√			
3.90	Branched Chain Hexane*				√		
4.56	Branched Chain Hexene*				√	√	
4.56	Dichloroethylene*	√	√	√	√		
4.65	Ethanol				√		
4.70	Isopropanol				√		
4.91#	Trimethyl Oxirane				√		
5.31	1-Chlorobutane			√			
5.48	2-Chloro-2-Methylbutane	√		√			
5.79	Cyclohexene		√		√		
6.02	Acetonitrile				√		
6.17	2-Butanone			√			
7.08	Hexyl Alcohol*			√		√	
7.19	Chloroform		√	√	√		

+ Peak co-eluting with solvent in Column 1
Peak co-eluting with solvent in Column 2
* Isomer not determined

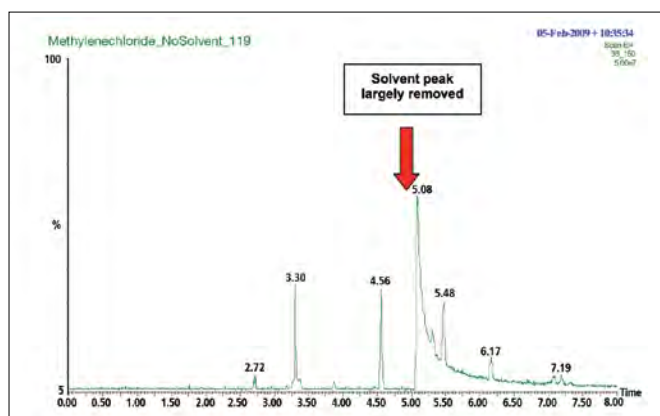


Figure 6. Chromatograms shown in Figures 4 and 5 plotted together at a larger scale to show the efficacy of sidecutting for solvent removal.

Although this sidecutting technique allows the sample to be processed on the MS without the potential damage and interference from the solvent peak, it does not take into account any peaks which will co-elute with the solvent on Column 1 – these peaks would not enter Column 2 or be seen by the MS.

Close examination of Figure 5 reveals that two peaks are missing from this chromatogram at approximately 3.42 and 3.67 minutes that were present in Figure 4. These clearly must co-elute on Column 1.

To enable these (and possibly other) peaks that co-elute with the solvent to be transferred to the second column for separation, a peak-sectioning technique was used to deliver time-incremented narrow heartcuts of the solvent peak from successive runs of the same DCM sample. Figure 7 (Page 5) shows how the solvent peak was sectioned into six 0.02-minute heartcuts. This approach allows the area under the solvent peak on Column 1 to be fully mapped by Column 2 without exposing the MS detector to large amounts of solvent.

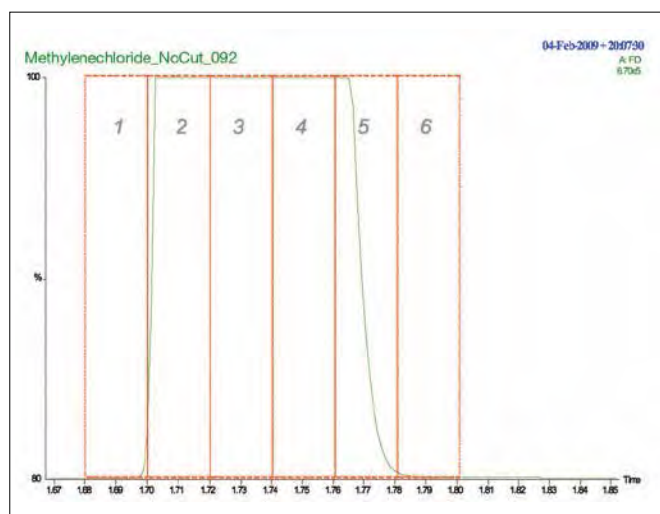


Figure 7. Sectioning the DCM solvent peak into six 0.02-minute heartcuts.

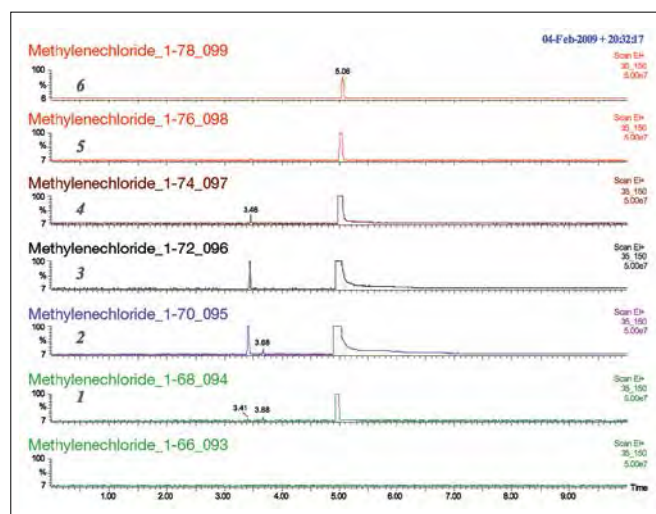


Figure 8. Chromatograms from successive 0.02-minute heartcuts.

Figure 8 shows the six chromatograms obtained from the successive solvent cuts. The 'lost' peaks at approximately 3.4 and 3.7 minutes are now apparently recovered.

In Figure 8, we have effectively delivered the whole solvent to the second column and have been able to prevent gross overloading of the column and the detector and are able to recover two components that would have been otherwise lost. By combining these data with those from Figure 5, we are able to provide a comprehensive result for the impurities in this type of sample without the associated problems of large solvent peaks. Table 3 shows the impurities identified in the five DCM samples using this technique. In all cases, the impurity peaks were well separated from the DCM peak.

The next sample examined was a batch of ethyl acetate that had significantly more impurities than the DCM samples previously examined.

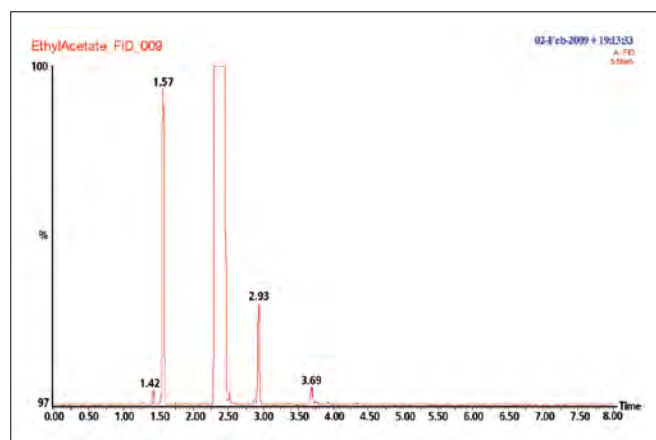


Figure 9. Sample of ethyl acetate on Column 1 and the FID.

Figures 9, 10, 11 and 12 (Pages 5-6) show the chromatography on the FID, the total sample on the MS, the sample with the solvent removed by sidecutting, and the heartcut-sectioned solvent peak respectively. Table 4 (Page 7) lists the compounds identified in this sample.

In this analysis, there are three peaks that elute with the solvent peak on Column 1: n-hexane, 1-chloro-2-methylpropane and 2-butanol.

What is also of particular interest from these data are the three peaks that elute between 5.00 and 5.30 minutes. These would co-elute with the solvent peak on Column 2 and so they would only be seen when the solvent is eliminated by sidecutting, as shown in Figure 11 (Page 6).

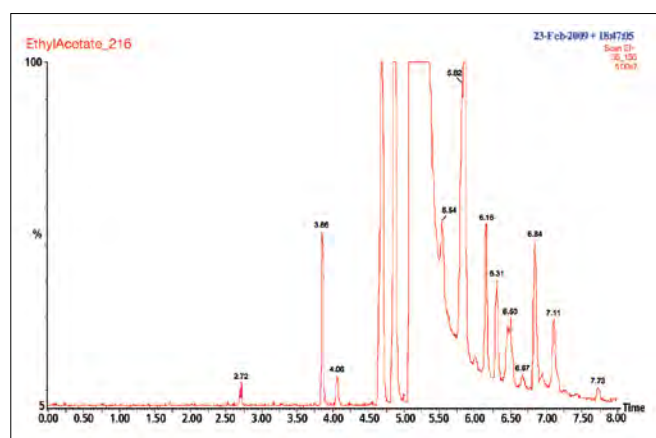


Figure 10. Chromatogram of total ethyl acetate sample transferred to Column 2 and the MS detector.

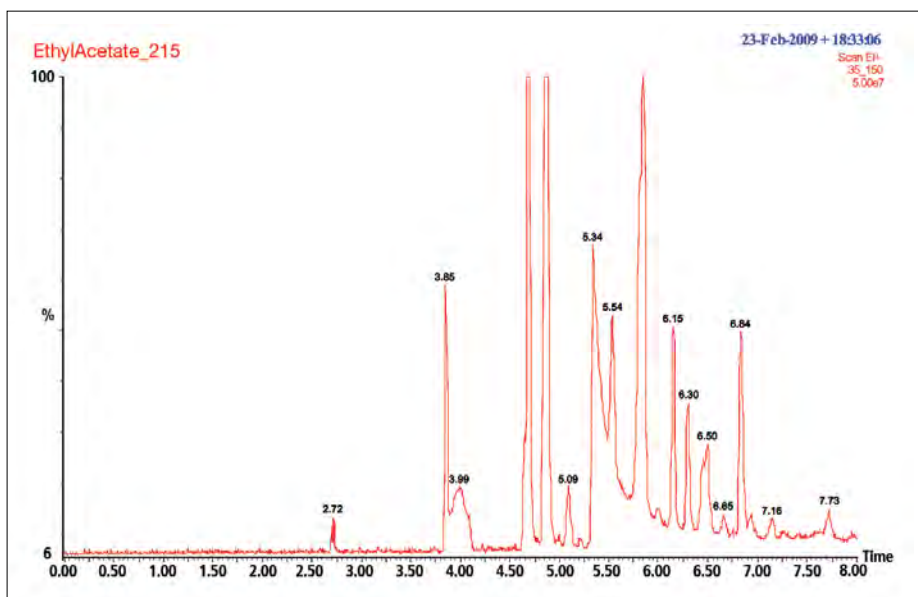


Figure 11. Chromatogram of ethyl acetate sample with the solvent removed by sidecutting on Column 2 and the MS detector.

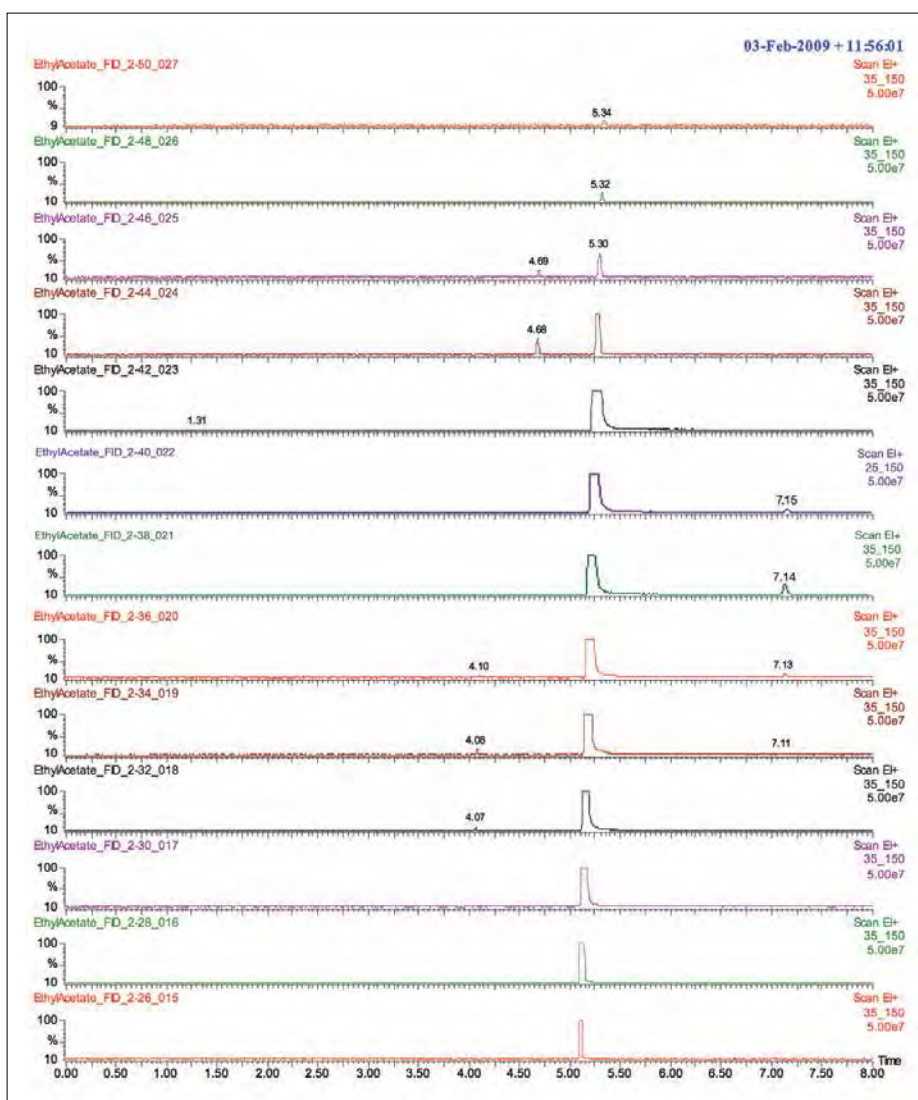


Figure 12. Ethyl acetate solvent peak sectioned by heartcutting into Column 2 and the MS.

Table 4. Tentative MS assignment of compound identities in ethyl acetate sample using the solvent sidecutting and heartcut sectioning technique.

Retention Time (min)	MS Identification
3.85	Acetone
4.06+	n-Hexane
4.65	Ethanol
4.68+	1-Chloro-2-Methylpropane
4.69	Isopropanol
4.86	1-Ethoxy-2-Methyl-Propane
5.01#	Dichloromethane
5.09#	2-Butanone
5.20#	Tetrahydrofuran
5.54	Branched Chain Octane*
5.75	n-Heptane
5.81	Isopropyl Acetate
5.85	1-Ethoxybutane
5.99	Branched Chain Nonane*
6.15	Pentanone*
6.30	1-Ethoxybutene
6.45	3-Methyl-2-Butanol
6.50	Isopropyl Propionate
6.65	Branched Chain Undecane*
6.84	1,2-Dimethoxypropane
6.94	Ethoxy Acetic Acid
7.13+	2-Butanol
7.16	2-Methylpropyl Formate
7.73	n-Propyl Acetate

+ Peak co-eluting with solvent in Column 1

Peak co-eluting with solvent in Column 2

* Isomer not determined

Conclusion

This sidecutting and heartcutting technique provides a comprehensive and reliable method for revealing the low-level impurities of solvents. Although the solvent-peak sectioning process entails several repeat chromatograms of the same sample, these runs are fairly short and isothermal, so the total analytical time is just 50 minutes. This time would be needed to fully map the obscured components. In the samples examined here, only two additional peaks were found in the sectioned chromatograms, so the method could be optimized just to apply heartcuts to the affected sections and so reduce the number of runs necessary.

Although we have shown the application of this technique just to samples of dichloromethane and ethyl acetate, the same approach could be extended to other solvents or any sample where there is an interest in identifying and quantifying compounds at low levels that co-elute with other relatively large peaks.

Thermal Analysis



Investigation of Amorphous Sucrose Using Material Pockets and Humidity Generator



Summary

Sucrose is a well known material used for a variety of applications. In its simplest form it is used as sugar in cooking or for coffee. It is also used as an excipient in some pharmaceutical preparations. This study shows how the amount of water present in a sugar sample will greatly affect its mechanical properties. Using the Triton Technology Humidity Controller linked to the PerkinElmer® DMA 8000, it is shown how the Tg of amorphous sucrose changes when exposed to relative humidity. In addition, a comparison of a very dry sample of sucrose with one exposed to lab atmospheric moisture is shown.

Introduction

Dynamic Mechanical Analysis (DMA) is one of the most appropriate methods to investigate relaxation events. This fact, until now, has not been exploited for powdered materials due to the difficulty in handling powders. Some work has been done with dilatometry, but with the development of the Material Pocket, it has become easier for powdered materials to be investigated in a DMA 8000.

DMA works by applying an oscillating force to the material and the resultant displacement of the sample is measured. From this, the stiffness can be determined and the modulus and $\tan \delta$ can be calculated. $\tan \delta$ is the ratio of the loss modulus to the storage modulus. By measuring the phase lag in the displacement compared to the applied force it is possible to determine the damping properties of the material. $\tan \delta$ is plotted against temperature and glass transition is normally observed as a peak since the material will absorb energy as it passes through the glass transition.

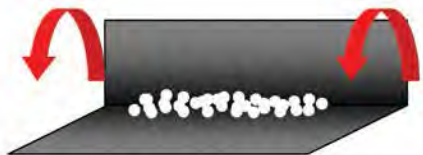
The following example shows sucrose to be very hygroscopic, at least in the initial adsorption of water. It also shows the effect of moisture on the glass transition temperature.

Experimental

Thermal scan of sucrose.

Approximately 50 mg of sucrose was loaded into a Material Pocket and the pocket was mounted in the DMA 8000. Three samples were investigated. (a) A very dry sample. (b) A dry sample exposed to laboratory atmosphere for 24 hours (c) Same as sample "b" but run at 50% RH.

Equipment	Experimental Conditions
DMA 8000	Sample: Spray dried sucrose
Fluid Bath	Geometry: Single Cantilever Bending
Humidity Generator	Support: Material Pocket
Circulator	Temperature: 20 °C to 200 °C at 5 °C min ⁻¹
	Frequency: 1.0 Hz
	Humidity: 0 and 50%



Results and conclusion

Figure 1 shows a simple thermal scan of the slightly damp sucrose sample. The experiment was performed at two frequencies. The initial peak at about 75 °C is frequency dependant indicating a relaxation, in this case the Tg. The second broader peak is not frequency dependant and can be attributed to the recrystallization of the amorphous material.

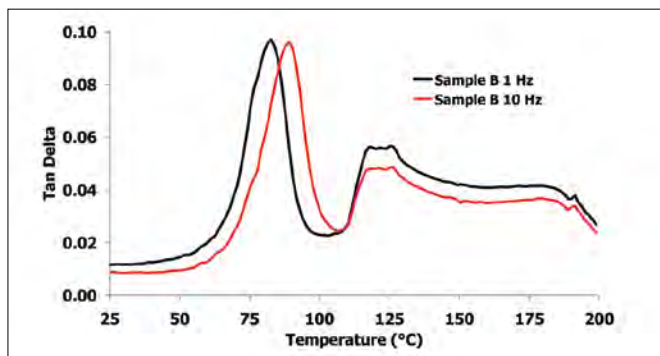


Figure 1. Thermal scan of damp sucrose sample.

The response when the relatively dry sample of sucrose was exposed to 50% relative humidity is shown in Figure 2. The $\tan \delta$ curve starts to increase as the sample is plasticized and the material starts going through its Tg. The temperature was chosen to be just below the Tg of the unhumidified sample (shown in Figure 1).

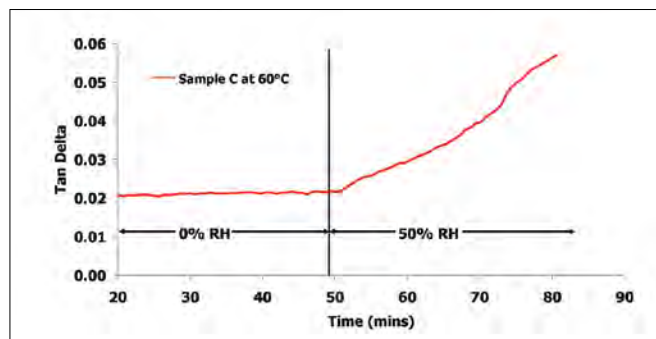


Figure 2. Dry sucrose sample exposed to 50% relative humidity.

Figure 3 shows the comparison between the three samples of sucrose. Sample A was very dry and shows the Tg at the highest temperature. Sample B was exposed to a modest amount of water and shows a small reduction in the Tg and Sample C was run while exposed to 50% relative humidity. A clear trend in the plasticizing of the material is observed as a decrease in Tg as a function of water exposure. The recrystallization peak is also shown to decrease as a function of water proving that this process is water mediated.

These data demonstrate that using the DMA 8000 in conjunction with the Material Pocket and the Humidity Controller can give information on the relaxation processes and the influence of water for amorphous powdered materials.

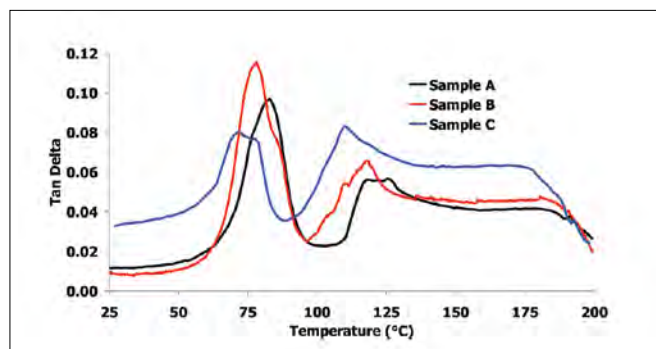


Figure 3. Comparison of all three sucrose samples.

FT-NIR Spectrometry

Author:

Justin Lang, PhD

Lauren McNitt

PerkinElmer, Inc.
Shelton, CT

Detection of Honey Adulteration Using FT-NIR Spectroscopy

Introduction

It is not uncommon to find high-value commodities such as foods to have compromised quality. These commodities can be adulterated by unscrupulous suppliers

to increase their profit margins. Unfortunately, it is often difficult to determine if products have been adulterated.

A high-value product commonly associated with adulteration is honey. Adding corn syrup allows dishonest suppliers to maintain the sweet taste without a noticeable difference in the product. Without testing, it is hard to tell which honeys are adulterated and which are not. Traditional testing methods for adulterated honey can be lengthy and expensive. Fraudulent mislabeling of honey is also a major problem. FDA guidelines for labeling of honey state:

- If a food contains only honey, the food must be named "honey".
- If a food contains honey and any other ingredients such as sweeteners it must be labelled accordingly, for example, "blend of honey and sugar".
- The floral source can be stated, such as Clover Honey.
- Any product that is not pure honey cannot be labeled as "honey."

Fourier Transform Near-Infrared Spectroscopy (FT-NIR) provides a quick, high quality testing method that allows for the detection of adulterants in honey. In order to optimize the effectiveness of the technique, various data modelling approaches were tested.

Data Analysis Approaches for Detection of Adulterants

The detection of adulterants in products can be either targeted or non-targeted. In targeted approaches, such as Partial Least Squares (PLS), the adulterant is a specific material that you are looking for within the product. This allows for a quantitative measurement of the amount of that adulterant, assuming a suitable calibration has been generated from a series of calibration standards. Each adulterant material will require a separate calibration. A typical non-targeted approach, such as Soft Independent Modelling of Class Analogies (SIMCA), will inform the analyst if the product does not conform to the expected material profile. It will indicate that the product may be adulterated, but it cannot say what it is adulterated with and by how much.

Spectrum 10's unique Adulterant Screen™ will inform the analyst when the product does not conform, identify the adulterant, and estimate the concentration of the adulterant without the lengthy requirement of running (multiple concentration) standards for each known adulterant and future adulterants. This allows for rapid deployment of initial Adulterant Screen methods and rapid method updating with new adulterants.

Experimental

NIR spectral data was collected on a PerkinElmer Frontier™ NIR spectrometer by pouring the honey sample into a Petri dish, placing the Petri dish onto the top of the NIRA II Reflectance Accessory, and placing a Transflectance Adaptor on top of the sample. Spectra were collected at 8 cm⁻¹ resolution using a scan time of 30 seconds.

Spectra of the following pure samples were measured:

- Clover honey
- Wildflower honey
- Orange blossom honey
- Organic honey
- Corn syrup
- Rice syrup

Ten replicate spectra were measured for each of these pure materials.

In addition, dilutions of the pure material using corn syrup were prepared yielding the following concentrations:

- Clover Honey
 - ♦ 0%, 2%, 4%, 6%, 8%, 10%, 12%, 14%, 16%, 18%, 20%, 30%, 40%, 50%, 60%, 70%, 80%, 90%, 92%, 94%, 96%, 98%, 100%
- Wildflower Honey
 - ♦ 0%, 20%, 40%, 60%, 80%, 100%
- Organic Honey*
 - ♦ 0%, 20%, 40%, 60%, 80%, 100%

Additional sample dilutions were prepared as validation samples to test the methods: The wildflower, orange blossom, clover, and organic honeys were diluted two separate times, once with 10% corn syrup and once with 10% rice syrup.

Results

Figure 1 contains the scans of three different samples with varying concentrations of honey (0% honey is Corn Syrup). There are clear spectral differences between the samples at these high concentrations. The second derivative (Figure 2) simplifies the view to quickly identify differences and will also remove any baseline offsets or slopes from the data.

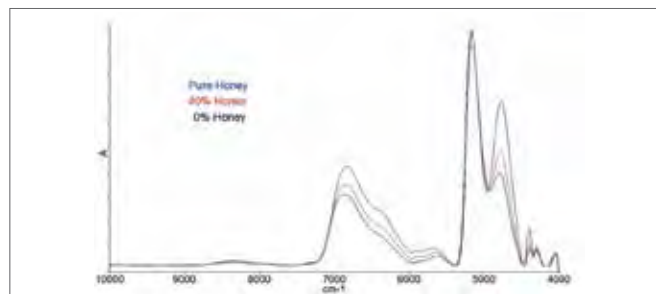


Figure 1. FT-NIR overlay demonstrating the typical spectra of honey.



Figure 2. Second derivative spectra of samples in Figure 1.

A PLS quantitative model was generated from the clover honey/corn syrup standard mixtures. Figure 3 shows the calibration for the NIR estimated concentration versus the specified mixture concentrations for these standards. The data shows an excellent correlation indicating that PLS modeling may be successful in characterizing honeys with “known” adulterants.

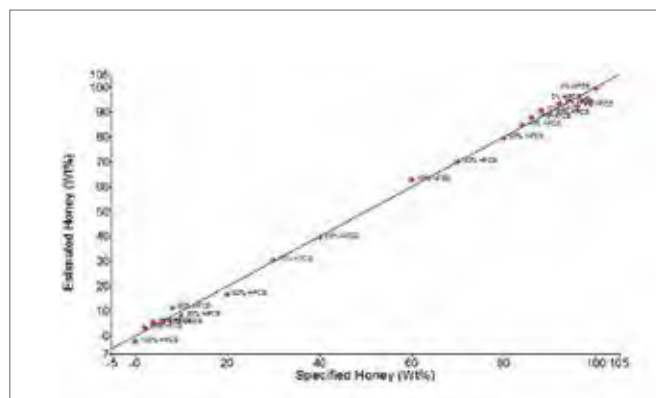


Figure 3. PLS model of honey dilutions with a line of best fit.

A further calibration was performed incorporating all of the standard mixtures from organic, clover, and wildflower honeys, shown in Figure 4. This calibration implies that the flower type has little impact for the samples and adulterants chosen in this model.

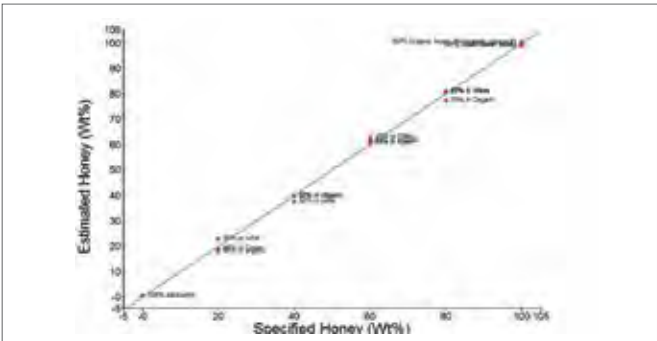


Figure 4. PLS model of three different honeys of the same dilution seen on the line of best fit.

Table 1. PLS result for honey validation sample.

	Validation Sample Concentration
Calculated Corn Syrup %	41.89 Wt%
Actual	41.25 Wt%
Difference	0.64

A validation sample of honey with known concentration of corn syrup, not included in the PLS model, was used to verify the honey calibration. Table 1 shows how the model quantified the unknown, with a difference of 0.64%.

A SIMCA model was generated by inputting 8 of the 10 replicate samples for each of the honeys using the spectral range 10,000-4,000 cm^{-1} , with 2nd derivative applied to the data. The remaining two replicates for each type of honey were used as an Independent Validation set along with a honey sample spiked with 10% of corn syrup.

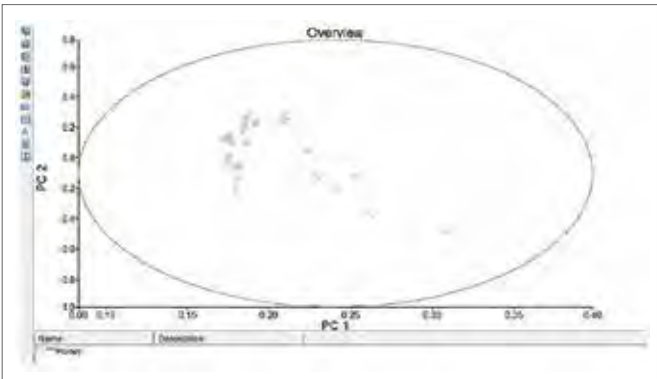


Figure 5. Principal Components plot for honey varieties.

Figure 5 shows the Principal Component (PC) plot of PC1 vs PC2 for the honey samples. All the clover, wildflower, and orange blossom honey spectra lay in within the boundary of the model. The results from the Independent Validation are shown in Figure 6.

	Sample ID	Specified Material	Identified Material	Result	Specified Material Total Distance Ratio
1	Clover honey 09	Honey	Honey	Passed	0.4034
2	Clover honey 10	Honey	Honey	Passed	0.5831
3	Wildflower Honey 09	Honey	Honey	Passed	0.6490
4	Wildflower Honey 10	Honey	Honey	Passed	0.6555
5	Orange Blossom Honey 09	Honey	Honey	Passed	0.5635
6	Orange Blossom Honey 10	Honey	Honey	Passed	0.7036
7	Honey Honey with 10% HFC5	Honey	Honey	Passed	0.7316

Figure 6. Independent validation results for honeys.

All of the replicate pure honey samples passed. However, the spiked sample also registered a pass result. The SIMCA method would require more work to try to determine an appropriate PASS/FAIL threshold.

An Adulterant Screen method was generated by inputting all of the pure honey spectra as “material spectra” and adding in high fructose corn syrup and rice syrup as “adulterant spectra”. First Derivative pre-processing was applied within the method. The SIMCA method and the Adulterant Screen method were implemented in a Spectrum Touch™ application allowing for sequential analysis using SIMCA, followed by Adulterant Screen. The sample spiked with 10% high fructose corn syrup was tested using this Spectrum Touch method, as shown in Figure 7.

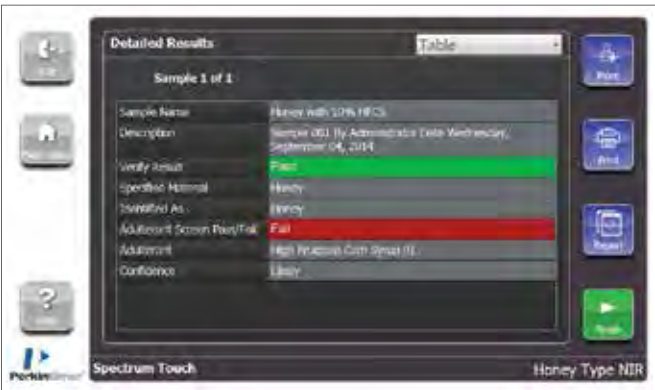


Figure 7. Results from Verify (SIMCA) and Adulterant Screen testing a 10% dilution of honey.

As detailed previously, the SIMCA analysis gives a false PASS result. However, Adulterant Screen correctly recognizes that the sample is adulterated with high fructose corn syrup.



Figure 8. Detailed view of results from the Adulterant Screen of a 10% dilution of honey.

Figure 8 shows the detailed Adulterant Screen results for a honey sample diluted with corn syrup. The results show the estimated percentage of high fructose corn syrup the model found in the sample. The line labeled 'Detection Limit' indicates the minimum detection limit (about 4%) of this adulterant using this method. Adulterants with significantly different spectra from honey would be detectable at much lower limits.

Conclusion

The data included in this application note indicates that it is possible to use NIR spectroscopy to detect adulteration of honey. NIR sampling is quick and easy. If the adulterant is known, then quantitative analysis of the adulterant can be achieved with PLS modeling. However, this requires the lengthy preparation of calibration standards. Adulterant Screen can detect adulteration with better sensitivity than a SIMCA model and can recognize which adulterant is present and estimate the adulterant concentration without quantitative calibration standards. Finally, the method can be deployed in a simple user interface to allow use by routine operators.

Liquid Chromatography

Authors:

Chi Man Ng

Wilhad M. Reuter

PerkinElmer, Inc.
USA

Analysis of Sugars in Honey Using the PerkinElmer Altus HPLC System with RI Detection

Introduction

Honey consumption has grown significantly during the last few decades due to its high nutritional value and unique flavor. The price of natural bee honey is much higher than other sweeteners making it susceptible

to adulteration with cheaper sweeteners, primarily sucrose. Besides lower levels of non-sugar ingredients, natural honey primarily consists of glucose and fructose and may contain low levels of sucrose and/or maltose.^{1,2} However, according to the international regulations, any commercially available "pure"-labeled honey products that are found to have in excess of 5% by weight of sucrose or maltose are considered to be adulterated.³

With the focus on possible honey adulteration, this application highlights the LC separation of various sugars found in honey and the analysis of these components in four store-bought honey samples. Method conditions and performance data, including linearity and repeatability, are presented.

Experimental

Hardware/Software

For all chromatographic separations, a PerkinElmer Altus™ HPLC system was used, including the Altus A-10 Solvent and Sample Module, Column Module, integrated vacuum degasser/ column oven and an Altus A-10 RI Detector. All instrument control, analysis and data processing was performed using the Waters® Empower® 3 CDS platform.

Method Parameters

The HPLC method parameters are shown in Table 1

Table 1. HPLC Method Parameters.

HPLC Conditions							
Column:	PerkinElmer Brownlee™ Analytical Amino 3 μm, 4.6 x 150 mm (Part# N9303505)						
Mobile Phase:	Solvent A: 65:35 acetonitrile/water Solvent program:						
	Time (min)	Flow Rate (mL/min)	%A	%B	%C	%D	Curve
	Initial	1.000	100.0	0.0	0.0	0.0	Initial
Analysis Time	6 min.						
Flow Rate:	1.0 mL/min. (2300 psi)						
Oven Temp.:	25 °C						
Detection:	Altus A-10 RI; cell temp.: 35 °C						
Injection Volume:	5 μL						
Sampling (Data) Rate:	10 pts./sec						

Solvents, Standards and Samples

All solvents and diluents used were HPLC grade and filtered via 0.45- μ m filters.

The sugar standards were obtained from Supelco® (Irvine, CA) and consisted of fructose, glucose, maltose and sucrose. Stock sugar standards were made using 65:35 acetonitrile/water as diluent. For the 1333 μ g/mL (ppm) stock solution, the standards were first dissolved in 17.5 mL of water before adding 32.5 mL of acetonitrile. The lower level standards were then prepared from this stock solution.

All commercially available honey products were purchased at local stores. They were labeled Honey W, Honey X, Honey Y and Honey Z. Each honey was prepared by dissolving 2.5 g into 50 mL of 65:35 acetonitrile/water, followed by another 1:1 dilution using the same solvent.

Prior to injection, all calibrants and samples were filtered through 0.45- μ m filters to remove small particles.

Results and Discussion

Figure 1 shows the chromatographic separation of the 1333- μ g/mL (ppm) sugar standard containing the four target sugars using the optimized conditions described above. The analysis time was under six minutes.

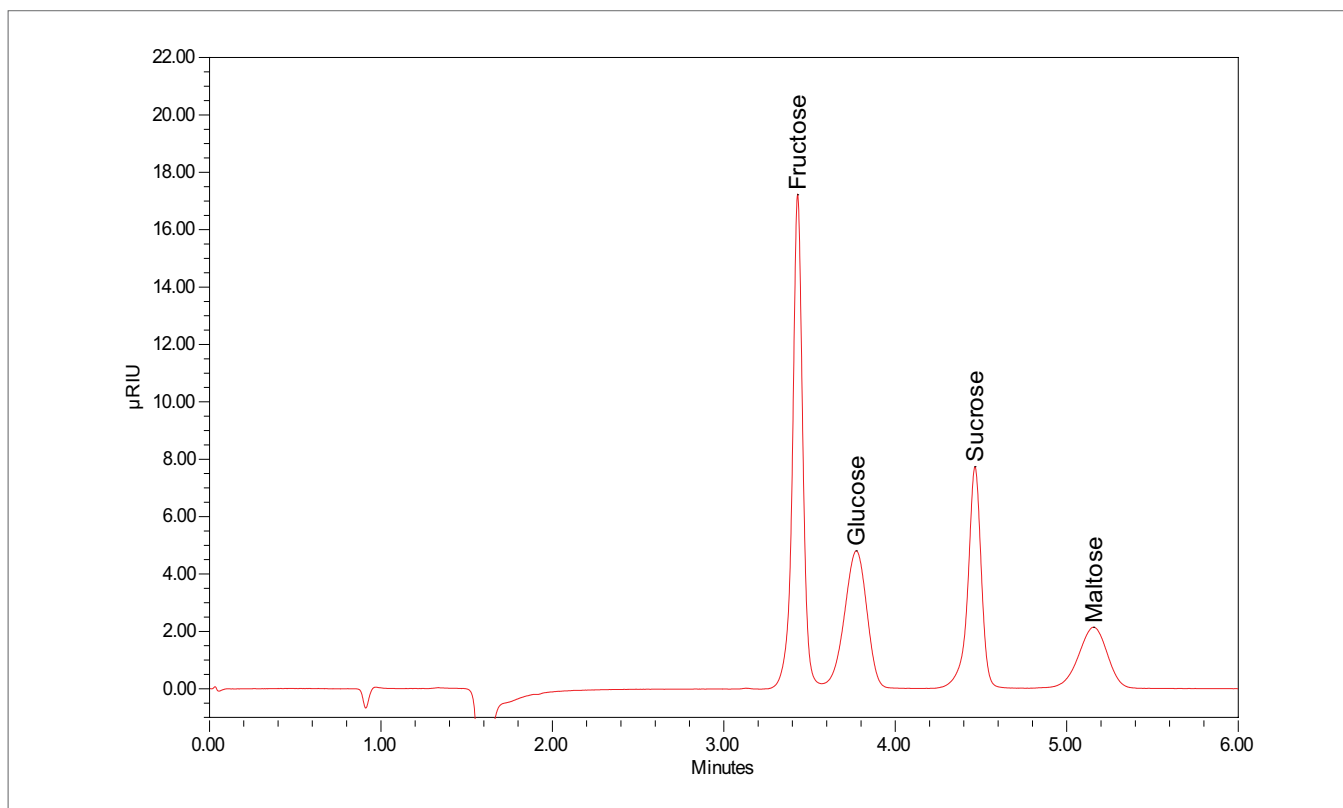


Figure 1. Chromatogram of the 1333 μ g/mL sugar standard.

Figure 2 shows the overlay of 12 replicate 667- $\mu\text{g/mL}$ sugar standard injections, demonstrating exceptional reproducibility. Retention time % RSDs were also quite exceptional, exemplified by 0.026% RSD for fructose.

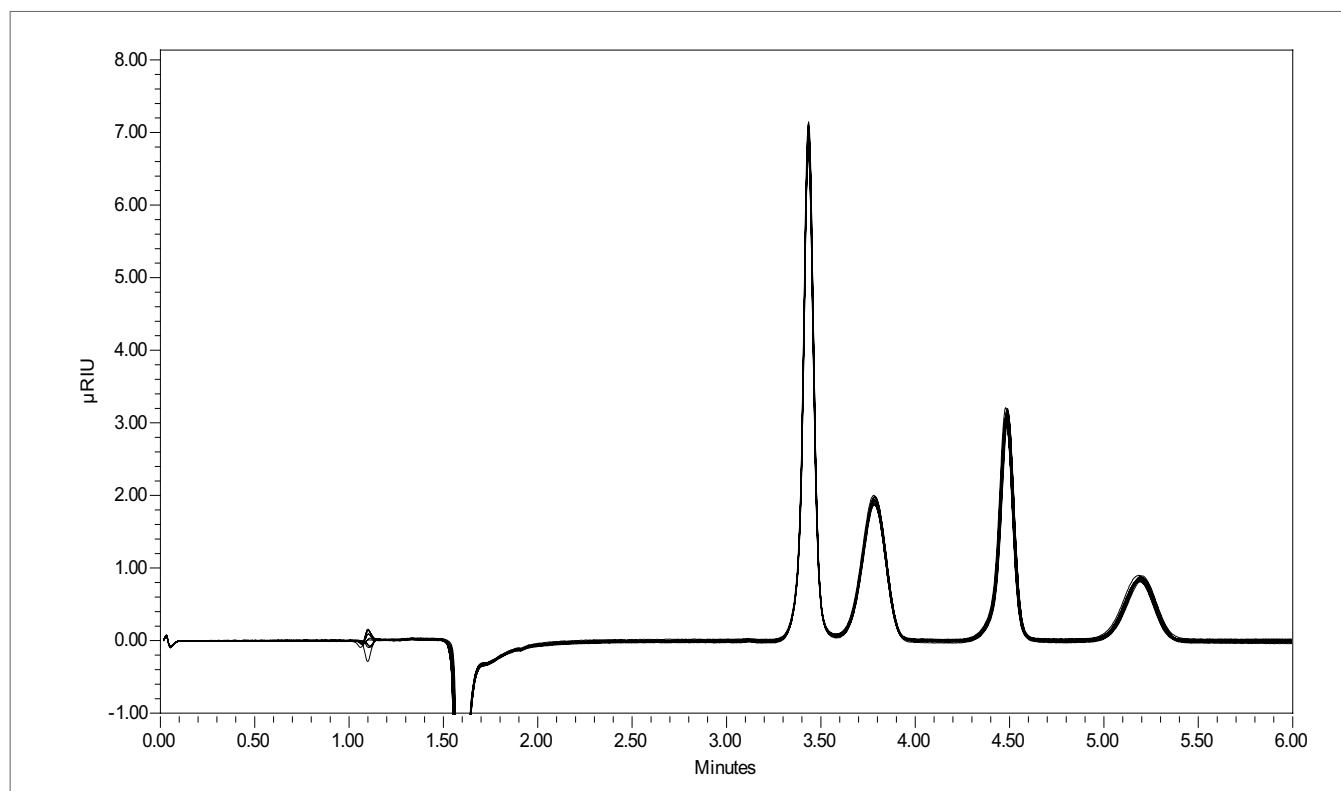


Figure 2. Overlay of 12 replicates of the 667 $\mu\text{g/mL}$ sugar standard.

Figure 3 shows the calibration results for all four sugars over a concentration range of 133 to 1333 $\mu\text{g/mL}$. All four sugars followed a quadratic (2nd order) fit and had R^2 coefficients > 0.999 ($n = 3$ at each level).

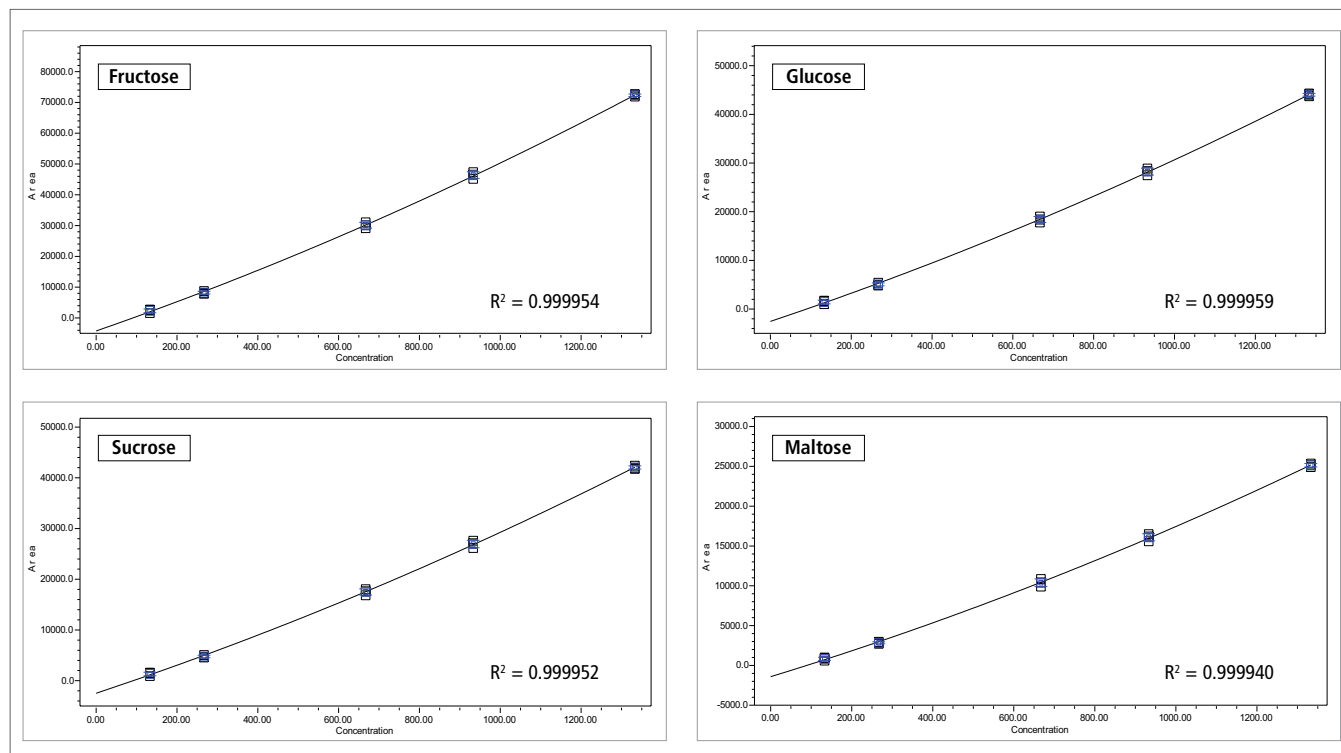


Figure 3. Results of 5-level calibration sets for fructose, glucose, maltose and sucrose.

Using the same chromatographic conditions, four honey samples were analyzed. The chromatographic results for Honey X, Honey Y and Honey Z are shown in Figure 4. Comparing the

chromatograms of these honey samples with the sugar standards, it can be observed that all three honey samples contain the same three sugars: fructose, glucose and small amounts of sucrose.

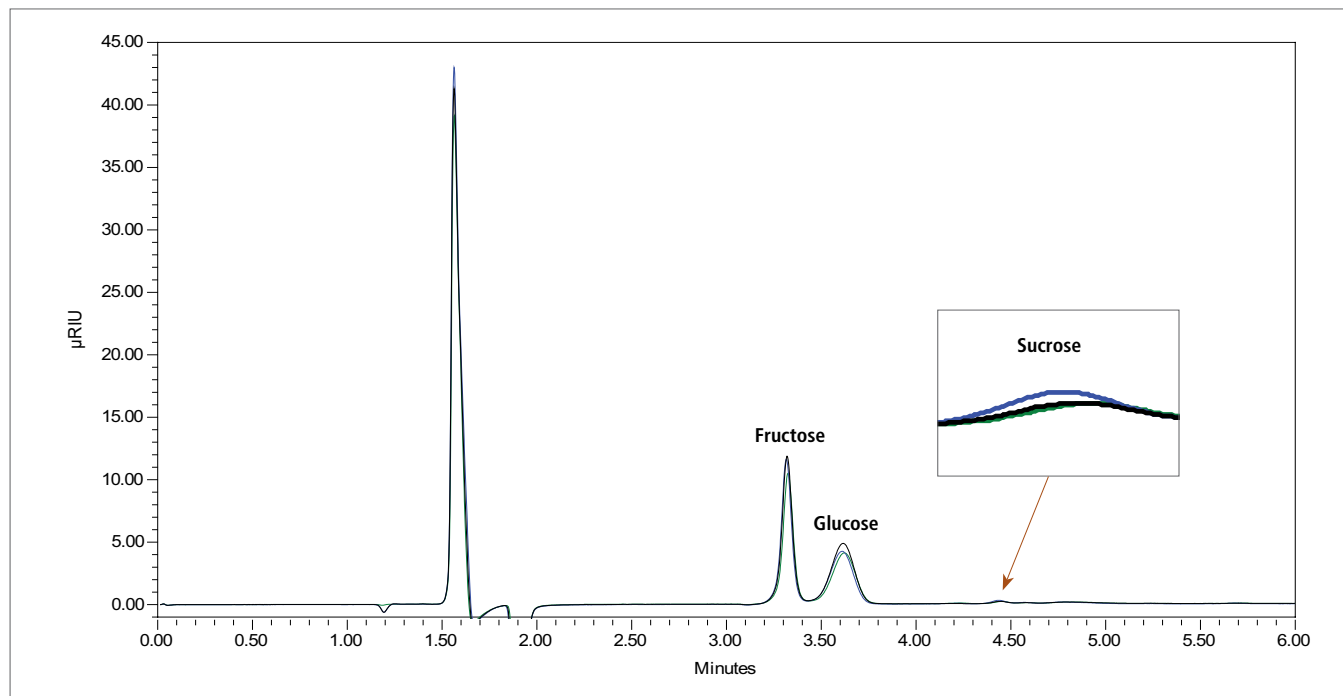


Figure 4. Overlaid chromatograms of Honey X (green), Honey Y (black) and Honey Z (blue).

Based on standard calibration, the quantitative results for each honey sample are shown in Table 2. Combining the fructose and glucose percentages for each honey sample, the overall fructose and glucose content for Honey X, Y, and Z was determined to be 50.90%, 57.13%, and 53.60%, respectively. These results are consistent with the accepted overall content of fructose and glucose in honey, expected to be somewhere around 60%.¹ The sucrose content for each honey sample was determined to be 3.20%, 3.26% and 3.90%, respectively. These values are all below the 5% mass ratio limit for sucrose that is allowed in unadulterated honey. Based on the data presented, the three store-bought honey samples do not appear to be adulterated with cheaper sweeteners.

Upon closer examination of the chromatogram of Honey W, a smaller but significant peak was observed at about 5.10 minutes (Figure 5). This matched the elution time for maltose in the standard mix. The amount of maltose was calculated to be 43.85 mg, and the percent sugar was calculated to be 1.75% (w/w). Considering the 5% (by weight) limit that is allowed in commercially available “pure”-labeled honeys, the resulting maltose level found in Honey W suggests it was not adulterated.

Table 2. Quantitative Results.

Honey X:		
Component	Amount (mg)	Percent Sugar (w/w)
Fructose	556.05	22.24
Glucose	716.48	28.66
Sucrose	79.875	3.20

Honey Y:		
Component	Amount (mg)	Percent Sugar (w/w)
Fructose	610.23	24.41
Glucose	817.95	32.72
Sucrose	81.525	3.26

Honey Z:		
Component	Amount (mg)	Percent Sugar (w/w)
Fructose	602.30	24.09
Glucose	737.78	29.51
Sucrose	97.525	3.90

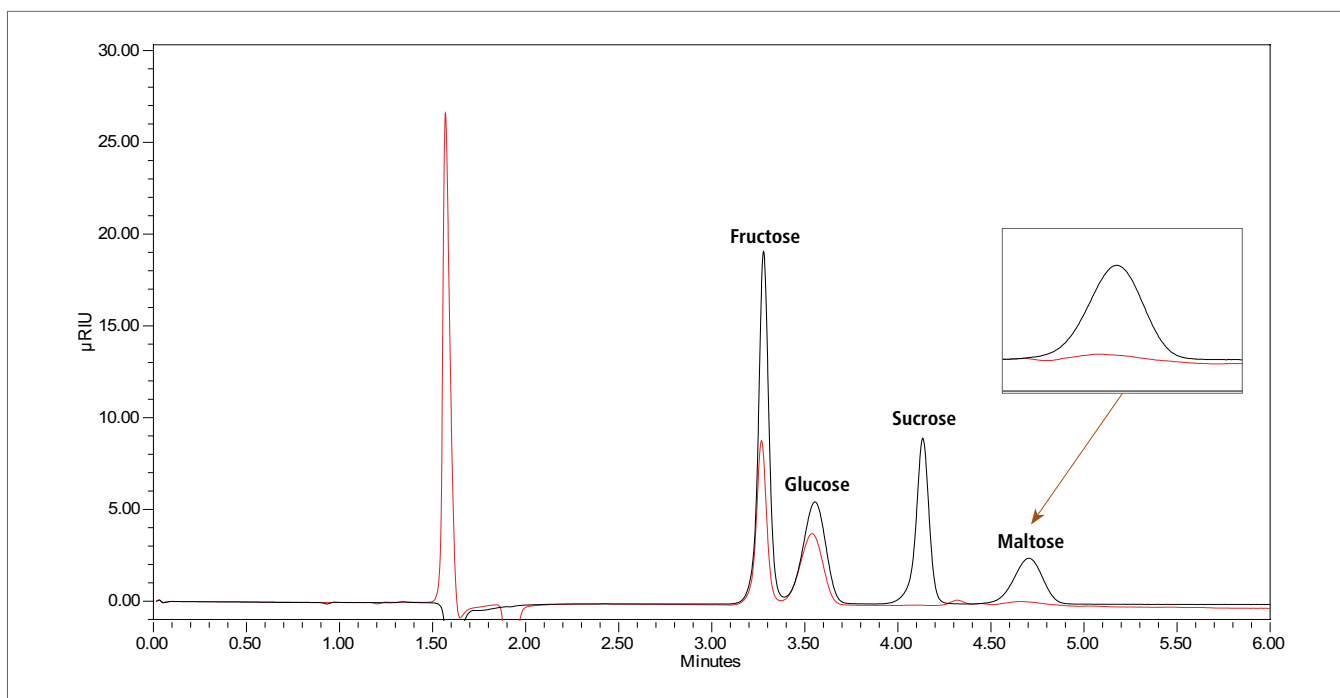


Figure 5. Overlay chromatograms of Honey W (red) and the 133 ppm sugar standard (black), zooming in on last eluting peak.

Conclusion

This work has demonstrated the effective chromatographic separation of four sugars using a PerkinElmer Altus HPLC System with RI detection. The results exhibited very good retention time repeatability as well as excellent linearity over the tested concentration ranges.

From a food quality perspective, there is an ever growing emphasis on food monitoring. This is especially the case pertaining to the adulteration of honey. With this in mind, this work focused on the sugar analysis of four store bought honeys, identifying the particular analytes contained in each of the honey samples, as well as comparing the sugar profiles, both chromatographically and quantitatively.

References

1. W. Guo, Y. Liu, X. Zhu and S. Wang, "Dielectric properties of honey adulterated with sucrose syrup", *Journal of Food Engineering*, pp. 1-7, 2011.
2. A. Moussa, D. Noureddine, A. Saad and S. Douichene, "The Relationship between Fructose, Glucose and Maltose Content with Diastase Number and Anti-Pseudomonal Activity of Natural Honey Combined with Potato Starch", *Organic Chemistry Current Research*, vol. 1, no. 5, pp. 1-5, 2012.
3. Codex Alimentarius Commission, 2001; GB18796-2005, 2005



Dynamic Mechanical Analysis

Authors

Dr. Frederick J. Warren
Dr. Paul G. Royall
Dr. Peter R. Ellis
Dr. Peter J. Butterworth

King's College London
London, UK

Dr. Ben Perston

PerkinElmer, Inc.
Shelton, CT USA

Characterizing the Hydrothermal Behavior of Starch with Dynamic Mechanical Analysis

Introduction

Starch is one of the primary sources of energy in the human diet, and is also used in a wide range of industrial processes, including brewing, bioethanol production, paper manufacture and in the production of biodegradable plastics.¹

Starch exists in plants in a granular form, the granules being between 1 and 100 μm in diameter, and has a complex semi-crystalline structure. Starch consists of two polymeric components: amylose, which is an essentially linear α (1 \rightarrow 4) linked glucose chain, and amylopectin, which is a branched polymer of α (1 \rightarrow 4) linked glucose chains interspersed with α (1 \rightarrow 6) branch points. The relative proportions of amorphous and crystalline material in the starch granule, and the arrangement of structure in the granule, have a significant bearing on the behavior of the starch and its response to hydrothermal treatments.²

One of the most important modifications of starch structure that occurs during processing of starch, for both food usage and industrial applications, is gelatinization. When heated in excess water, starch goes through a thermal transition, termed gelatinization, at temperatures between 50 and 70 °C. Starch gelatinization is an endothermic transition associated with rapid swelling of the granule and melting of crystalline regions. In the absence of water, starch crystallites go through a melting transition at much higher temperatures

of around 150-170 °C. It is thought that the swelling of the amorphous regions of the starch granules, as they absorb water, introduces structural stress to the crystalline lamellae, allowing the crystallites to melt at a much lower temperature.

During gelatinization, “granule ghosts” (expanded, highly hydrated amorphous remnants of starch granules) are formed and large amounts of α -glucan material may be leached into solution. This large structural change may be used to characterize the gelatinization transition of a particular starch sample. However, the analysis is complicated by the significant degree of phase separation of the solubilized glucan chains and the granule ghosts. This phase separation renders starch gelatinization unsuitable for study in conventional cone-and-plate or plate-plate rheometers, because the native (un-gelatinized) starch granules will sink, creating a concentration gradient in the same direction as the direction of shear. This makes it impossible to obtain reliable estimates for the rheological properties of starch before and during gelatinization accompanying hydrothermal treatment. The rheological changes that occur to starch during gelatinization are important to understand for a range of industrial applications, for example in starches used as a filler to provide texture in the food industry, and as a potential predictor of the starches behavior as an enzyme substrate.

Dynamic mechanical analysis (DMA) is a technique ideally suited to the investigation of relaxation events, and is often used for determination of glass transition temperatures in polymers and other amorphous materials, e.g. amorphous lactose and composite materials. DMA works by applying an oscillating force (stress) to the sample and measuring the resultant displacement (strain). From these measurements, the storage modulus, loss modulus and phase angle ($\tan \delta$; equal to the ratio of the loss and storage moduli) can be calculated. The phase angle gives information about the damping properties of the material: $\tan \delta$ is plotted against temperature, and glass transitions are normally observed as a peak, since the material will absorb energy as it passes through the glass transition (a temporary increase in the loss modulus).

However, despite DMA’s advantages, until recently it has not been widely used for powdered and granular materials due to the difficulty in handling them in mechanical tests. The Material Pocket for the DMA 8000 instrument from PerkinElmer was developed to allow straightforward, reproducible analysis of powders with DMA. The Material Pocket is capable of supporting 20-50 mg of granular or powdered material in a pocket formed by a piece of folded steel. The pocket is manufactured from stainless steel, which is mechanically inert over a wide range of temperatures, and hence any transitions that are observed during heating are due to changes in the material held in the pocket. The bulk

of the mechanical response comes from the pocket, but any perturbations seen in the signal will result from transitions in the material held within the pocket.

An additional requirement for many applications, such as starch gelatinization and other transitions of food and pharmaceutical materials, is the ability to conduct powder DMA experiments in the presence of liquid water or more complex aqueous systems, since such situations model the processing end point for many powders that are heated in water and/or consumed by man. In this application note, we explore the use of immersion-mode material pocket DMA as a tool to investigate the structural changes associated with starch gelatinization.

Experimental

Wheat starch (Cerestar, cv. GL04) and pea starches (WT, *r* and *lam*) were gifts from Prof. T. Bogracheva and Prof. C. Hedley (formerly of the John Innes Centre, Norwich, UK). WT pea starch is a wild type pea starch comprising of ~30% amylose and 70% amylopectin (dry w/w). The *r* mutant pea starch has a mutation at the *rugosa* gene locus, which results in a starch with a very high (~70%) amylose content, because of a decreased activity of granule-bound starch synthase 1.³ The *lam* mutant starch has a mutation at the *low amylose* gene locus and contains only ~10% amylose.⁴ Potato starch was obtained from National Starch and Chemicals (UK). Waxy rice starch (cv. Remyrise) was a gift from Dr. P. Rayment (Unilever, UK) and is essentially free of amylose. Normal maize starch (cv. Globzeta) was a gift from Prof. I. Rowland (University of Reading, UK).

All experiments were carried out using a PerkinElmer DMA 8000 fitted with a water bath accessory. The sample was loaded into a stainless steel material pocket (PerkinElmer, Seer Green, UK, Part No. N5330323) with dimensions of 30 mm by 14 mm. The pocket was scored lengthways to allow it to be folded in half and folded to an angle of approximately 60° to allow sample loading. Approximately 30 mg of starch was accurately weighed into the pocket, and either loaded dry, or mixed with 50 μ L of water to make a slurry. The pocket was then folded in half, crimped closed to form a sandwich approximately 0.5 mm wide, reweighed, and clamped into the DMA. The pocket was loaded in a single cantilever bending mode, with one end of the pocket clamped to a fixed support and the other end clamped to the drive shaft. All the clamps were tightened using a torque wrench to a force of 5 N. This meant that one end of the pocket was held stationary, while the other end was subjected to an oscillating displacement by the driveshaft. This resulted in the pocket being deformed in an oscillating, bending motion in and out of plane, subjecting the starch powder (or slurry) in the pocket to a horizontal shear.

The samples were submerged in a water bath containing ~100 mL of deionized water, and subjected to heating from 20 °C to 90 °C at a heating rate of 1 °C/min (or placed in a dry air oven using the same heating conditions), while undergoing a dynamic displacement of 0.05 mm at 1, 10 and 30 Hz. The force was automatically controlled between 1 N and 10 N to achieve the target displacement. The modulus was calculated from the actual measured dynamic displacement amplitude.



Figure 1. The DMA 8000 dynamic mechanical analyzer with immersion bath accessory.

Results and Conclusions

In the absence of water, starch does not go through a gelatinization transition. When starch was loaded as a dry powder into a material pocket and subjected to heating in a standard dry air oven, no transitions were observed between ambient temperature and 90 °C.

In order to induce a gelatinization transition, starch was loaded as a slurry with water in a material pocket, which was then closed with sealant. When this sample was heated from ambient to 90 °C, a small transition was observed at ~60 °C, near the gelatinization point of the starch. However, repeat runs showed poor reproducibility, with the temperature and intensity of the transition varying widely. This lack of reproducibility was attributed to variations in the degree of hydration of the sample.

Subsequently, a dry sample of starch was placed in the material pocket, and submerged in ~100 mL of water in the DMA 8000 immersion bath attachment. The starch sample was then heated from ambient to 90 °C. The gelatinization peak was again observed, but suffered from the same poor reproducibility. Inspection of the sample after analysis revealed that air bubbles had formed in the material pocket, leading to incomplete, uneven hydration of the starch. Finally, loading the material pocket with starch slurry prior to immersion in the water bath led to good reproducibility in both the measured modulus and phase angle. Typical results are shown in Figure 2.

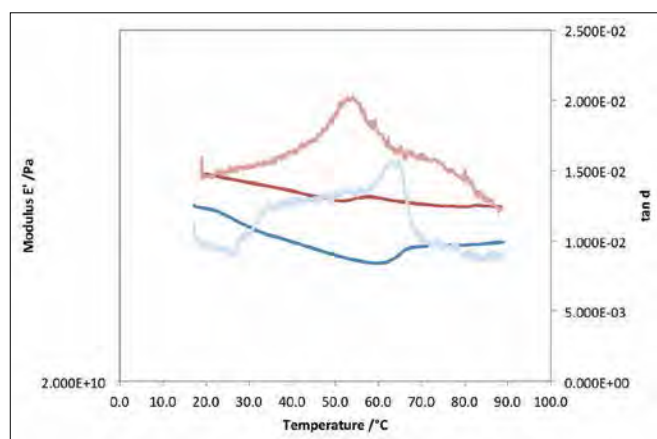


Figure 2. Tan δ (Maize – light blue, Wheat – light red) and modulus (Maize – dark blue, Wheat – dark red) values for starch slurries heated in the material pocket by immersion mode DMA.

The peaks seen in the modulus and tan δ for DMA analysis of starch in the material pocket clearly relate to structural changes in the starch that occur during gelatinization, which can also be observed by DSC and polarized light microscopy (Figure 3). The tan δ peak clearly correlates with the gelatinization onset temperature as measured by DSC and with the initial swelling of some granules (and loss of birefringence) observed with polarized light microscopy (Figure 3). No frequency dependence is observed for the tan δ , so it can be concluded that this is not a glass transition. A likely explanation for the tan δ peak is that it arises from the water absorption and swelling of the granules that occurs in the first stages of gelatinization.

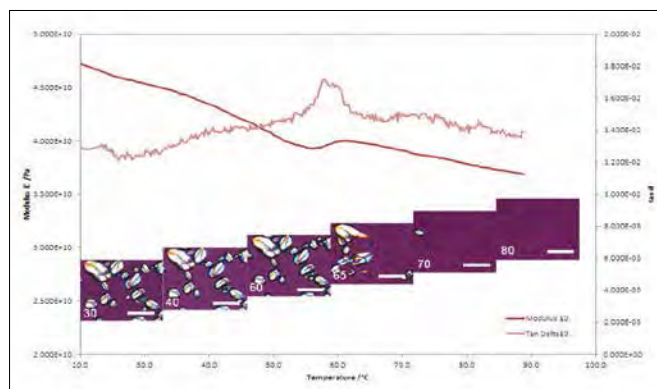


Figure 3. Tan δ (light red) and modulus (dark red) responses for potato starch heated in immersion mode DMA. Overlaid are polarizing microscopy images of potato starch suspended in water undergoing gelatinization. Temperatures are provided in °C. The scale bar represents 100 μm .

The modulus peak is observed at a temperature 5-6 °C higher than the $\tan \delta$ peak, at a temperature corresponding to the peak in the DSC gelatinization endotherm (Table 1 and Figure 4). The modulus peak also shows no frequency dependence. This peak may be interpreted as resulting from the near simultaneous relaxation in the amorphous regions of the starch granule and melting of crystalline regions that occurs during gelatinization.

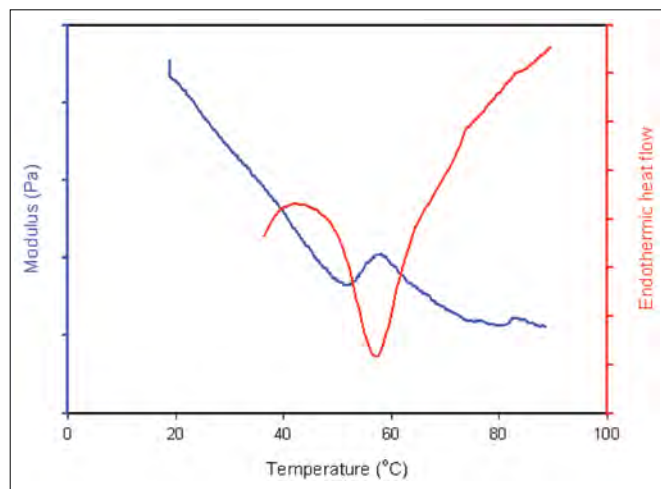


Figure 4. Modulus values for wheat starch heated in immersion mode DMA (blue) overlaid with endothermic heat flow for wheat starch in excess water measured by DSC (red).

The natures of the peaks that are observed for starch gelatinization by DMA are dependent on the type of starch that is used. Starches with very low (<10% w/w) amylose content have smaller $\tan \delta$ and modulus peaks, reflecting the smaller change in viscosity on gelatinization. This is at least in part because amylose leaching into solution is one factor in increasing the viscosity of the aqueous phase. Starches with very high amylose contents (>60% w/w) fail to show peaks, as these starches do not go through major structural changes during gelatinization.

For more a more detailed discussion see Warren, et. al. (2012).⁵

In conclusion, DMA is a tool that may be used to measure structural changes in starch due to hydrothermal treatment. DMA is capable of accurately measuring changes in starch structure associated with both the onset ($\tan \delta$) of gelatinization, and the main gelatinization transition (modulus). The DMA offers more flexibility than alternative methods (e.g. DSC) as more awkward samples may be loaded into the material pocket, and the environment around the sample may be far better controlled. Using the water bath and humidity unit available with the PerkinElmer DMA 8000, sample behavior may be investigated under a wide range of humidity values, and immersed in a range of aqueous or non-aqueous liquids. This great flexibility and control make the DMA 8000 a powerful tool for characterisation of starch under a range of conditions not available with other techniques.

Table 1. Peak temperatures in the $\tan \delta$ and modulus peaks for starch gelatinization, measured at 30Hz. Where data could be reliably obtained in triplicate, values are presented as means of triplicates (\pm s.e.m). Otherwise values are from single readings. DSC onset and peak gelatinization temperatures are presented as means of triplicates (\pm s.e.m.). Amylose contents of starch samples (% w/w) determined by iodine binding are presented as means of triplicates (\pm s.e.m.)

Starch Type	$\tan \delta$ Peak (°C)	Modulus Peak (°C)	DSC Onset Temp. (°C)	DSC Peak Temp. (°C)	Amylose Content (% w/w)
Wheat	52.8 (± 2.0)	57.7 (± 0.6)	49.3 (± 0.2)	57.2 (± 0.2)	22.8 (± 0.3)
Maize	59.9 (± 2.3)	65.9 (± 2.0)	64.3 (± 0.2)	70.0 (± 0.0)	22.8 (± 2.2)
Waxy rice	58.5	66.3	57.3 (± 0.1)	67.2 (± 0.4)	1.2 (± 0.1)
Potato	60.3 (± 0.5)	64.4 (± 2.0)	59.6 (± 0.0)	65.0 (± 0.0)	15.3 (± 1.6)
r pea	N.D.*	N.D.*	43.9 (± 1.1)	70.0 (± 2.9)	65.1 (± 1.3)
lam pea	60.9 (± 2.9)	68.8	62.8 (± 0.1)	67.0 (± 0.2)	7.0 (± 0.1)
Wild type pea	53.9 (± 1.3)	57.7 (± 0.4)	52.9 (± 0.1)	59.0 (± 0.0)	31.9 (± 0.3)

*N.D. Not determined

References

1. Jobling, S. (2004). Improving starch for food and industrial applications. *Current Opinion in Plant Biology*, 7, 210-218.
2. Buléon, A., Colonna, P., Planchot, V., and Ball, S. (1998). Starch granules: structure and biosynthesis. *International Journal of Biological Macromolecules*, 23, 85-112.
3. Lloyd, J.R., Hedley, C.L., Bull, V.J., and Ring, S.G. (1996). Determination of the effect of *r* and *rb* mutations on the structure of amylose and amylopectin in pea (*Pisum sativum* L.). *Carbohydrate Polymers*, 29, 45-49.
4. Wang, T.L., Bogracheva, T.Y., and Hedley, C.L. (1998). Starch: As simple as A, B, C? *Journal of Experimental Botany*, 49, 481-502.
5. Warren, F.J., Royall, P.G., Butterworth, P.J., and Ellis, P.R. (2012). Immersion mode material pocket dynamic mechanical analysis (IMP-DMA): a novel tool to study gelatinization of purified starches and starch-containing plant materials. *Carbohydrate Polymers under review*.



APPLICATION NOTE

Gas Chromatography/ Mass Spectrometry

Author

Ruben Garnica

Andrew Tipler

PerkinElmer, Inc.
Shelton, CT 06484 USA

Qualifying Mustard Flavor by Headspace Trap GC/MS using the Clarus SQ 8

Mustard is a common condiment used across many cultures and culinary styles to enhance the dining experience. It is derived from the mustard seed and is used either as a dried spice, spread or paste when the dried spice is mixed with water, vinegar or other liquid. The characteristic sharp taste of mustard arises from the isothiocyanates (ITCs) present as result of enzymatic activity made possible when the ground seed is mixed with liquids. The focus of this application brief is the characterization of these ITCs by headspace trap gas chromatography/mass spectrometry (GC/MS) and a qualitative description of their relationship to sharpness in taste across various mustard products.

Method

The experimental conditions for this analysis are given in Tables 1 to 4. The vials used are the standard 22-mL vials with aluminum crimped caps with PTFE lined silicon septa.

Table 1. GC Conditions.

Gas Chromatograph Clarus® 680	
Column	60 m x 0.25 mm x 1.0 µm Elite-SMS
Oven	35 °C for 5 min, then 6 °C/min to 245 °C
Injector	Programmable Split Splitless (PSS), 180 °C, Split OFF
Carrier Gas	Helium at 2.0 mL/min (28.6 psig initial pressure), HS Mode ON

Table 2. HS Trap Conditions.

Headspace System TurboMatrix™ 110 HS Trap	
Vial Equilibration	80 °C for 20 minutes
Needle	120 °C
Transfer Line	140 °C, long, 0.25 mm i.d. fused silica
Carrier Gas	Helium at 31 psig
Dry Purge	7 min
Trap	CarboPack C, 25 °C to 260 °C, hold for 7 min
Extraction Cycles	1 @ 40 PSI

Table 3. MS Conditions.

Mass Spectrometer Clarus® SQ 8S	
Scan Range	35 to 350 Daltons
Scan Time	0.1 s
Interscan Delay	0.06 s
Source Temp	180 °C
Inlet Line temp	200 °C
Multiplier	1700V

Table 4. Sample Details.

Sample	Sample Weight (g)
Mustard Seed (ground)	0.50
British Mustard Powder (dry)	0.50
British Mustard Powder (reconstituted)*	1.00
British Mustard	1.00
French Mustard	1.00

*reconstituted per manufacturer instructions

Results

The total ion chromatogram obtained from French and British mustard samples are given in Figure 1. These intensity locked spectra demonstrated the higher level of ITCs present in British mustard as indicated by the larger peaks for allyl isothiocyanate (RT = 21.00 min) and 4-isothiocyanato-1-butene (RT = 24.28 min). This difference is indicative of the sharp versus smooth taste between British and French mustard.

The large presence of ITCs shown in Figure 1 is contrasted with the total ion chromatogram obtained from ground mustard seed given in Figure 2. In general ground mustard seed lacks volatile flavor compounds because the enzymatic activation with liquid has not been performed. Figure 3 demonstrates this activation with a comparison between dry British mustard powder and a reconstituted sample. In these labeled total ion chromatograms the intensity scales are locked between the spectrum and it is clear that activation with water has drastically increased ITC level in the reconstituted paste. The component identities were established by performing mass spectral library searches with the best match presented here. Peaks labeled with a single asterisk indicate detector overloading while peaks labeled with a double asterisk indicate inconclusive compound identification due to structural similarities.

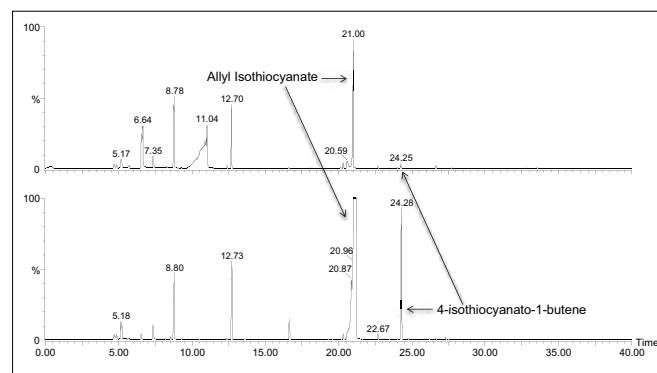


Figure 1. Full total ion chromatogram obtained from French (top) and British (bottom) mustards.

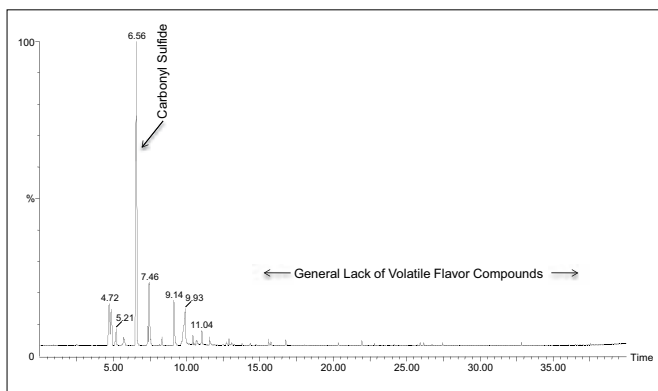


Figure 2. Full Total Ion Chromatogram obtained from mustard seed sample.

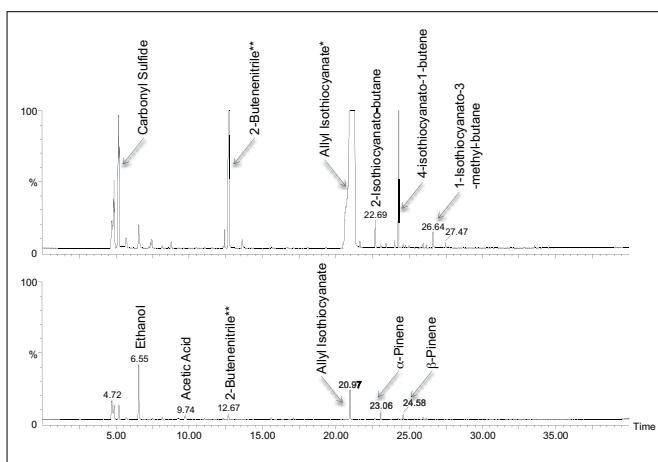


Figure 3. Full total ion chromatogram obtained from British mustard powder (bottom) and reconstituted British mustard powder (top).

Conclusions

This system provides a very simple and convenient way of characterizing the volatile flavor components of mustard based products. A rapid comparison between production samples may be made to monitor the enzymatic activation process and help producers arrive at the correct sharpness in taste. The combination of HS Trap with GC/MS allows for component detection at low-level concentration combined with the mass spectral compound identification.

FT-IR Spectroscopy**Author:**

Justin Lang, PhD

Lauren McNitt

PerkinElmer, Inc.
Shelton, CT

The Use of FT-IR Spectroscopy as a Technique for Verifying Maple Syrup Authenticity

Introduction

Although usually not thought of until pancakes or waffles are on the table, maple syrup is a serious

business. It is one of the key crops where demand is greater than supply. Surprisingly, it takes 10 gallons of sugar maple tree sap to produce one quart of maple syrup. Because the syrup produced is only 1/40th of the actual sap yield, unscrupulous syrup suppliers are tempted to fraudulently adulterate their products with lower value commodities, in order to maximize their profit. Adulterants include cane syrup, high fructose corn syrup, beet syrup, and rice syrup. Infrared spectroscopy is shown here to be a fast and easy technique for detection and identification of these adulterants.

Method

Samples of Grade A maple syrup, corn syrup, high fructose corn syrup, and rice syrup were analyzed on the PerkinElmer Frontier™ Fourier Transform Infrared (FT-IR) spectrometer from 4,000 to 650 cm^{-1} , using a three-bounce Universal Attenuated Total Reflectance (UATR) sampling accessory. Samples were scanned by placing a single drop directly onto the diamond crystal of the UATR. After scanning, the UATR was cleaned using isopropyl alcohol on a laboratory wipe. Seven replicate measurements were performed for each sample type using a fresh aliquot for each scanned sample. Additional dilutions of maple syrup with the adulterants were prepared and scanned in order to validate the method.

Spectra of maple syrup and two of the common adulterants are shown in Figure 1A and an expanded region of interest in Figure 1B.

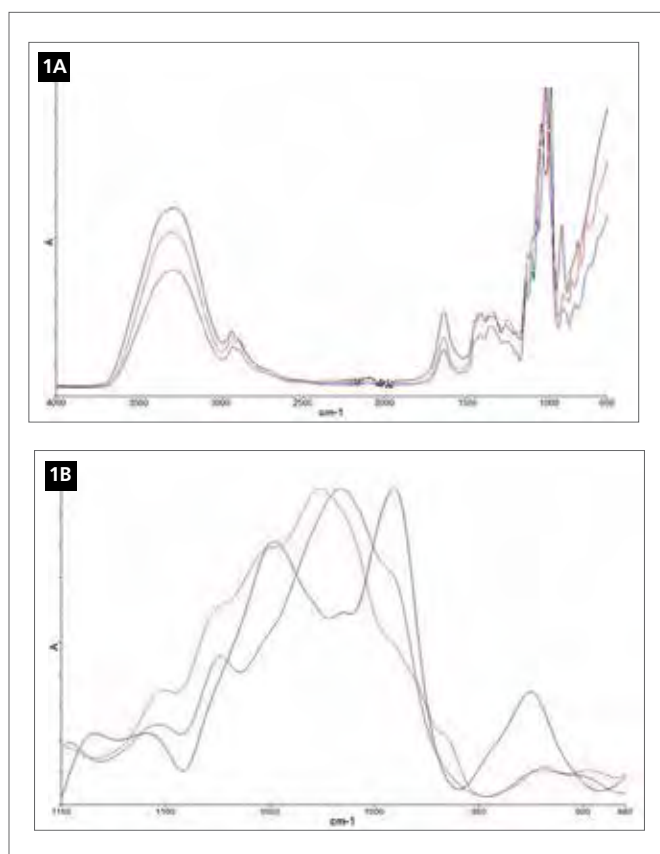


Figure 1A. FT-IR overlay of maple syrup and its common adulterants. maple syrup (black), high fructose corn syrup (red), rice syrup (blue). Figure 1B. Expanded spectral overlay of maple syrup (black), rice syrup (blue), and high fructose corn syrup (red), from 1150-880 cm^{-1} .

The spectra of these materials exhibit differences particularly in the spectral region from 1100 - 900 cm^{-1} .

A Soft Independent Model by Class Analogy (SIMCA) model was created to see if there was a measureable difference between the maple syrup and the adulterants. The SIMCA model is shown as Figure 2.

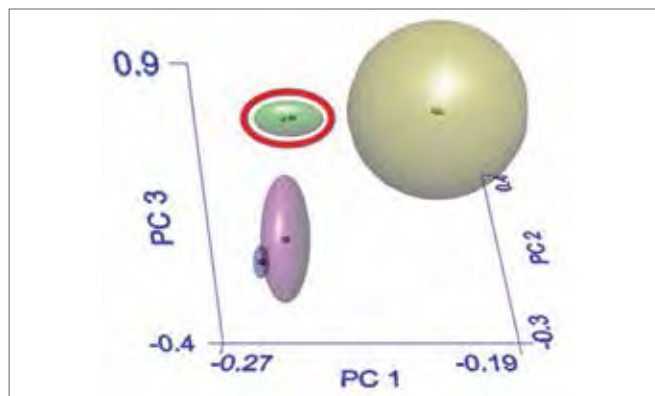


Figure 2. SIMCA model for the maple syrup and adulterants dataset (maple syrup highlighted).

There is good separation between maple syrup and the other adulterants, with a little overlap between the corn syrup and rice syrup. This model could be used to determine if the sample of interest is a maple syrup or not.

An Adulterant Screen™ method was set up using all of the maple syrup spectra as “Material Spectra” and single spectra of the adulterants as the “Adulterant Spectra”. A Spectrum Touch™ method was set up incorporating the SIMCA model and the Adulterant Screen method into a simple user interface for the routine analyst. The model and method were tested using one of the diluted samples, 10% high-fructose corn syrup in maple syrup. The Spectrum Touch results screen is shown as Figure 3.



Figure 3. Spectrum Touch results screen.

This test sample fails both the SIMCA and the Adulterant Screen analysis. SIMCA indicates that this test sample does not conform to the maple syrup spectra in the model and Adulterant Screen states that adulteration is likely with high fructose corn syrup.



Figure 4. Spectrum Touch results screen highlighting the “Adulterant Screen details” view.

The Adulterant Screen results not only predict which adulterant is present, it will also predict how much of that adulterant is present and estimate its detection limit. This is achieved without the need for the lengthy process of preparing and measuring spectra of calibration standards. In this case, Adulterant Screen predicts a concentration level for the high-fructose corn syrup adulterant at 9.737%, very close to the actual concentration of 10%.

Conclusion

As maple syrup is a prime target for food fraud, there is a clear need to test for its authenticity. It has been demonstrated that utilizing an FT-IR empowered method with Adulterant Screen and SIMCA allows for the measurement of maple syrup quality and detects any adulterants that may be present. The advantage of Adulterant Screen is that it only requires base materials for the method and is fast and easy to use. This dramatically reduces the time required to develop a screening method as quantitative calibration development is not required. Additional adulterants can readily be added into Adulterant Screen without having to recalibrate the method.

References

- <http://www.mi-maplesyrup.com/education/facts.htm>
- <http://tapmytrees.com/copsap.html>

Liquid Chromatography**Author:**

Wilhad Reuter

PerkinElmer, Inc.
Shelton, CT

The Qualitative and Quantitative Analysis of Steviol Glycosides by HPLC-PDA in Energy/Vitamin Drinks

Introduction

With an emphasis on decreasing calorie intake, more and more individuals are focusing on lowering their sugar consumption from foods and beverages.

In response to this, food/beverage manufacturers are now introducing the highly touted sugar substitute rebaudioside A (Reb A), in place of all or most of the sugar in certain foods and beverages. The primary interest in Reb A is the fact that it is a naturally derived sweetener considered to be at least 400 times sweeter than sugar and, therefore, can be added to products in considerably lower concentrations. The use of Reb A has been especially accelerated now that it is considered as *Generally Recognized as Safe* (GRAS) by the U.S. FDA¹. Reb A and stevioside, both steviol glycosides, are the primary extracts from the *Stevia rebaudiana* plant from South America, particularly from Paraguay. Along with Reb A and stevioside, two secondary steviol glycosides, rebaudioside B (Reb B) and rebaudioside C (Reb C), may also be introduced into food/beverage products as part of the stevia extracts, though both of these are not as sweet.

As the use of stevia extracts as sweeteners has gained significant momentum, due to its limited availability, there is a growing concern of both adulteration and label claim accuracy in products reported to contain these extracts. With the above in mind, this application highlights the HPLC separation of Reb A, stevioside, Reb B and Reb C, as well as the analysis of these components in a selection of three energy/vitamin drinks. The chromatographic conditions were so chosen as to closely match the latest monograph covering steviol glycosides, including the four listed above, published by the Joint FAO/WHO Expert Commission on Food Additives (JECFA)². This monograph, specifying the use of HPLC and a UV-based detector, is considered the internationally recognized method for analyzing steviol glycosides in food and beverage products. The USP monograph for Reb A closely parallels the JECFA monograph, though the USP's chromatographic method prescribes a more complex gradient approach³. Following the JECFA protocol, 210 nm was chosen as the analytical wavelength since steviol glycosides adequately absorb only in this region.

Experimental

Hardware/Software

For all chromatographic separations, a PerkinElmer Flexar™ Binary HPLC system (binary pump, autosampler, vacuum degasser and column oven) was used. Detection was accomplished using a PerkinElmer Flexar PDA Plus™ photodiode array detector and a 50 mm flow cell. All instrument control, analysis and data processing was done via PerkinElmer Chromera™ software.

Method Parameters

The HPLC method parameters are shown in Table 1.

Table 1. HPLC Method Parameters

HPLC Conditions	
Column	PerkinElmer Brownlee™ 5 µm 250 x 4.6 mm Validated C18 (Part# N9303561)
Mobile Phase	32% acetonitrile 68% 10 mM Na ₂ HPO ₄ buffer; pH 2.7 with phosphoric acid
Analysis Time	25 min.
Flow Rate	1.0 mL/min.
Oven Temp	40 °C
Detection	Flexar PDA Plus at 210 nm; Bandwidth = 5
Injection Volume	5 µL

Solvents, Standards and Samples

All solvents and diluents used were HPLC grade and filtered via 0.45 µm filters. All steviol glycoside standards were obtained from ChromaDex® Inc. (Irvine, CA). These included rebaudioside A (Reb A), rebaudioside B (Reb B), rebaudioside C (Reb C) and stevioside. All standard dilutions were made using 30:70 acetonitrile/water.

Samples included three different energy/vitamin drinks labeled X, Y and Z, purchased at a local grocery store. As drink X was expected to contain a significantly higher concentration of Reb A, drink X was first diluted 1:1 with 30:70 acetonitrile/water. Drinks Y and Z were injected neat. Before injection, all samples and standards were first filtered via 0.45 µm filters to remove small particles.

Results and Discussion

Figure 1 shows the high level standard chromatogram of Reb A, stevioside, Reb C and Reb B, eluting in that order. This 200/100 ppm standard contained 200 ppm Reb A and 100 ppm for the other three analytes. From this stock solution, six additional serial dilutions were made, down to a 1.0/0.5 ppm standard.

A small impurity (IP) was noticed eluting just after Reb B. For quantitative accuracy, where detectable, this impurity was exponentially skimmed off as part of Reb B integrations.

Figure 2 shows the overlay of six replicate 200/100 ppm standard injections, demonstrating the exceptional reproducibility that can be expected.

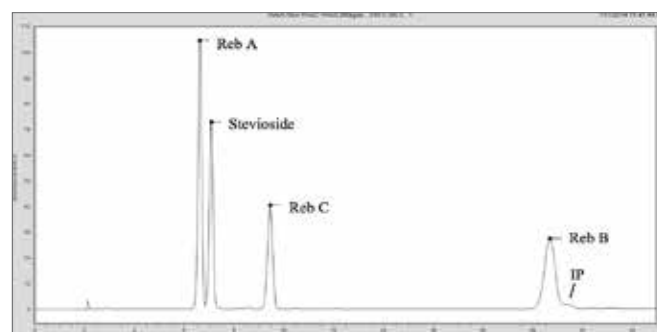


Figure 1. Chromatogram of upper level standard (200/100 ppm); IP = impurity peak.

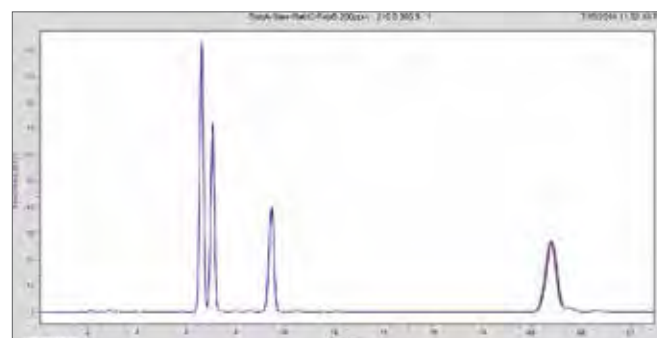


Figure 2. Overlay of six replicate 200/100 ppm standard injections.

Figure 3 shows the lower level standard (1.0/0.5 ppm) for these analytes. Based on these results, using a S/N limit of 10/1, the LOQs (limit of quantitation) for these analytes were calculated to be 0.5, 0.4, 0.6 and 0.7 ppm, respectively. Two additional matrix peaks ("MP") were detected but not identified. These peaks' individual spectral profiles were all considerably different from that of steviol glycosides.

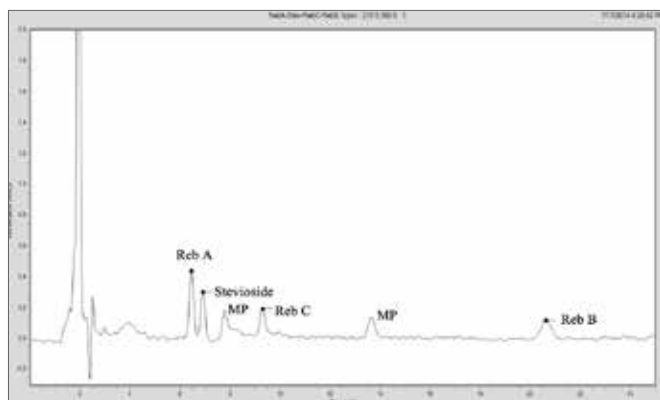


Figure 3. Chromatogram of lower level standard (1.0/0.5 ppm). MP = matrix peak.

Using Reb A and stevioside as examples, Figure 4 shows the linearity over the 1.0/0.5 ppm to 200/100 ppm concentration range, respectively. Both were found to be exceptionally linear within their ranges. It should be noted that the upper concentrations were chosen to accommodate the expected high-end concentrations within the analyzed samples and that the actual upper limit of linearity may be higher.

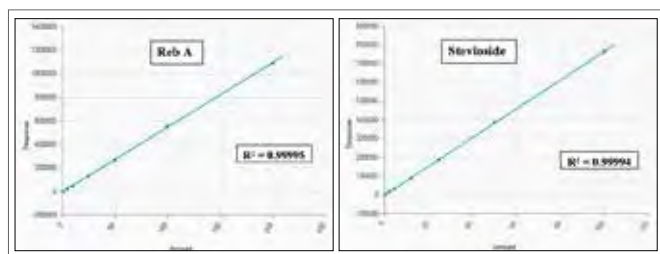


Figure 4. Linearity plots of Reb A (1.0-200 ppm) and stevioside (0.5-100 ppm).

Subsequently, using the same chromatographic conditions, three energy/vitamin drinks were analyzed: drink X, drink Y and drink Z. The resulting chromatogram for drink X (1:1 dilution; red) is shown in Figure 5, overlaid upon the 200/100 ppm standard (black). Thereupon, drink X appears to contain predominately Reb A with just a small amount Reb B. This is consistent with the label claim, which lists Reb A as a significant ingredient. The quantitative results are listed in Table 2. An additional matrix peak ("MP") was detected but not identified, though this peak's spectral profile was considerably different from that of steviol glycosides.

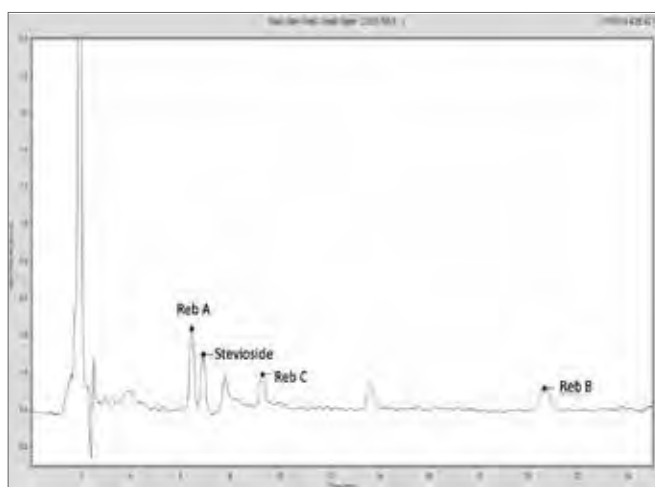


Figure 5. Chromatogram of Drink X diluted 1/1 with 30:70 acetonitrile/water (red) overlaid with 200/100 ppm standard (black).

Figure 6 shows the chromatographic result for drink Y (neat; red) overlaid upon the 25/12.5 ppm standard (black). In this case, there appears to be a slight retention time shift as compared to the standard. This was possibly due to a matrix effect. To further confirm peak identity, drink Y was spiked with standard, by diluting drink Y 1:1 with the 5/2.5 ppm standard. Per Figure 7, the resulting chromatogram shows a perfect overlay of the common analytes, confirming the retention time shift to be a matrix effect. Based on these results, drink Y was shown to contain predominantly Reb A and stevioside, with a smaller amount of Reb C. This is also consistent with the label claim for drink Y to contain steviol extract. The quantitative results are listed in Table 2. Four additional matrix peaks ("MP") were detected but not identified. These peaks' individual spectral profiles were all considerably different from that of steviol glycosides.

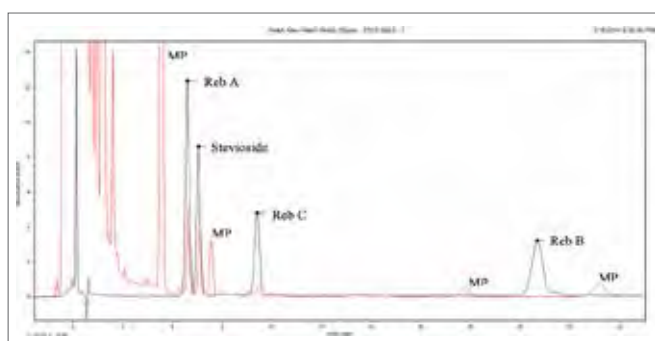


Figure 6. Chromatogram of drink Y (red) overlaid with 25/12.5 ppm standard (black).

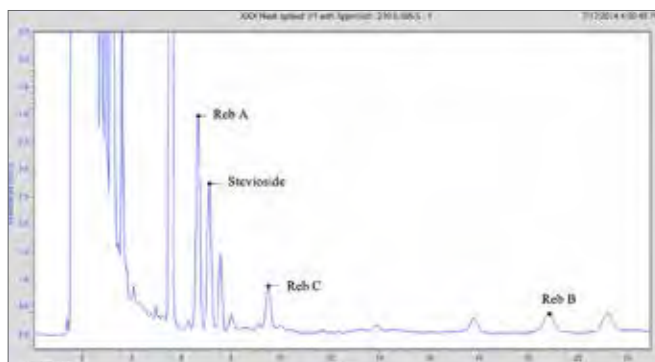


Figure 7. Chromatogram of drink Y spiked 1/1 with 5/2.5 ppm standard.

The resulting chromatogram for drink Z (neat; red) is shown in Figure 8, overlaid with the 25/12.5 ppm standard (black). From the overlay, it can be seen that none of the four steviol glycosides are detected. This was to be expected, as drink Z's label claim made no mention of containing any steviol glycosides. The two matrix peaks ("MP") that were detected in drink Z were not identified, though these peaks' individual spectral profiles were considerably different from that of steviol glycosides.

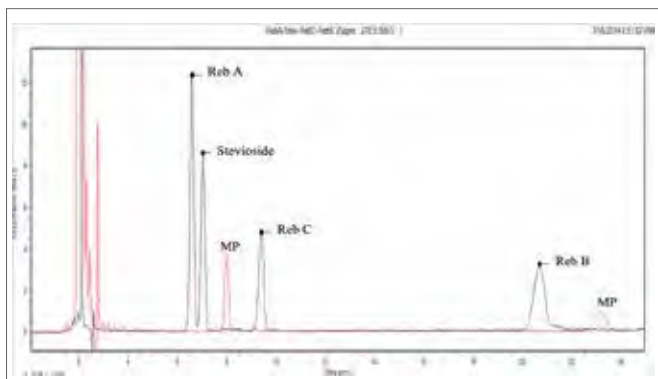


Figure 8. Chromatogram of drink Z (red) overlaid with 25/12.5 ppm standard (black). MP = matrix peak.

Table 2. Quantitative results for drinks X, Y and Z.

Component	Drink X Conc. (ppm)**	Drink Y Conc. (ppm)	Drink Z Conc. (ppm)
Reb A	286.2	9.2	ND
Stevioside	ND	4.7	ND
Reb C	ND	2.0	ND
Reb B	4.4	ND	ND

ND = not detected; ** = adjusted for 1:1 dilution

Per Table 2, as compared to drink Y, the amount of Reb A is appreciably higher in drink X. This is actually not that surprising, as the label claim for drink X reports zero sugar content while drink Y is supplemented with just over 5% sugar. As supported by the results, drink X is sweetened solely via Reb A.

Also, as listed in Table 2, drink Z contained no detectable steviol glycosides, which is consistent with the label claim.

Conclusion

This work has demonstrated the effective chromatographic separation of four steviol glycosides using a PerkinElmer Flexar HPLC-PDA Plus Chromera system. The results exhibited excellent retention time repeatability as well as exceptional linearity over the tested concentration ranges.

From a food quality perspective, there is an ever growing emphasis on food monitoring. This is especially the case pertaining to sugar substitutes. With this in mind, this work also focused on the steviol glycoside analysis of three energy/vitamin drinks, identifying the particular analytes contained in each drink, as well as comparing the three drinks' similarities and differences, both chromatographically and quantitatively.

References

1. U.S. FDA Agency Response Letter to GRAS; Notice # GRN 000253, 2008
2. Monograph on Steviol Glycosides, prepared at 73rd JECFA (2010) and published in FAO JECFA Monographs (2010)
3. Monograph on Rebaudioside A, Food Chemicals Codex, USP, Washington, DC, 2014

PerkinElmer, Inc.
940 Winter Street
Waltham, MA 02451 USA
P: (800) 762-4000 or
(+1) 203-925-4602
www.perkinelmer.com



For a complete listing of our global offices, visit www.perkinelmer.com/ContactUs

Copyright ©2015, PerkinElmer, Inc. All rights reserved. PerkinElmer® is a registered trademark of PerkinElmer, Inc. All other trademarks are the property of their respective owners.